Reformulation of the covering and quantizer problems as ground states of interacting particles

S. Torquato*

Department of Chemistry, Princeton University, Princeton, New Jersey 08544, USA;
Department of Physics, Princeton University, Princeton, New Jersey 08544, USA;
Princeton Center for Theoretical Science, Princeton University, Princeton, New Jersey 08544, USA;
Program in Applied and Computational Mathematics, Princeton University, Princeton, New Jersey 08544, USA;
and Princeton Institute for the Science and Technology of Materials, Princeton University, Princeton, New Jersey 08544, USA

(Received 6 September 2010; published 11 November 2010)

It is known that the sphere-packing problem and the number-variance problem (closely related to an optimization problem in number theory) can be posed as energy minimizations associated with an infinite number of point particles in d-dimensional Euclidean space $\mathbb{R}^d$ interacting via certain repulsive pair potentials. We reformulate the covering and quantizer problems as the determination of the ground states of interacting particles in $\mathbb{R}^d$ that generally involve single-body, two-body, three-body, and higher-body interactions. This is done by linking the covering and quantizer problems to certain optimization problems involving the "void" nearest-neighbor functions that arise in the theory of random media and statistical mechanics. These reformulations, which again exemplify the deep interplay between geometry and physics, allow one now to employ theoretical and numerical optimization techniques to analyze and solve these energy minimization problems. The covering and quantizer problems have relevance in numerous applications, including wireless communication network layouts, the search of high-dimensional data parameter spaces, stereotactic radiation therapy, data compression, digital communications, meshing of space for numerical analysis, and coding and cryptography, among other examples. In the first three space dimensions, the best known solutions of the sphere-packing and number-variance problems (or their "dual" solutions) are directly related to those of the covering and quantizer problems, but such relationships may or may not exist for $d \geq 4$, depending on the peculiarities of the dimensions involved. Our reformulation sheds light on the reasons for these similarities and differences. We also show that *disordered* saturated sphere packings provide relatively thin (economical) coverings and may yield thinner coverings than the best known lattice coverings in sufficiently large dimensions. In the case of the quantizer problem, we derive improved upper bounds on the quantizer error using sphere-packing solutions, which are generally substantially sharper than an existing upper bound in low to moderately large dimensions. We also demonstrate that *disordered* saturated sphere packings yield relatively good quantizers. Finally, we remark on possible applications of our results for the detection of gravitational waves.

DOI: 10.1103/PhysRevE.82.056109 PACS number(s): 89.90.+n, 05.20.−y, 89.20.Ff, 89.70.−a

I. INTRODUCTION

There are certain scientific problems that provide deep connections between many different scientific fields. The study of the low-energy states of classical interacting many-particle systems is an exemplar of a class of such problems because of its manifest importance in physics, materials science, communication theory, cryptography, mathematics, and computer science. Such many-particle systems have been used with great success to model liquids, glasses, and crystals when quantum effects are negligible [1,2]. The total potential energy $\Phi_N(\mathbf{r}^N)$ of N identical particles with positions $\mathbf{r}^N \equiv \mathbf{r}_1, \mathbf{r}_2, \ldots, \mathbf{r}_N$ in some large volume in d-dimensional Euclidean space $\mathbb{R}^d$ can be resolved into separate one-body, two-body, etc., N-body contributions:

$$\Phi_N(\mathbf{r}^N) = \sum_{i=1}^{N} u_1(\mathbf{r}_i) + \sum_{i<j}^{N} u_2(\mathbf{r}_i,\mathbf{r}_j) + \sum_{i<j<k}^{N} u_3(\mathbf{r}_i,\mathbf{r}_j,\mathbf{r}_k) + \cdots + u_N(\mathbf{r}^N), \tag{1}$$

where u_n represents the intrinsic n-body interaction in excess to the interaction energy for $n-1$ particles. To make the statistical-mechanical problem more tractable, the exact many-body potential (1) is usually replaced with a mathematically simpler form. For example, in the absence of an external field (i.e., $u_1=0$), often one assumes pairwise additivity, i.e.,

$$\Phi_N(\mathbf{r}^N) = \sum_{i<j}^{N} u_2(\mathbf{r}_i,\mathbf{r}_j). \tag{2}$$

Pairwise additivity is exact for hard-sphere systems and frequently has served to approximate accurately the interactions in simple liquids, such as the well-known Lennard-Jones pair potential [1], and in more complex systems where the pair potential u_2 in Eq. (2) can be regarded to be an *effective* pair interaction [3].

An outstanding problem in classical statistical mechanics is the determination of the *ground states* of $\Phi_N(\mathbf{r}^N)$, which are those configurations that globally minimize $\Phi_N(\mathbf{r}^N)$ and hence are the states that exist at absolute zero temperature. While classical ground states are readily produced by slowly freezing liquids in experiments and computer simulations, our theoretical understanding of them is far from being complete [4,5]. Virtually all theoretical and computational

*torquato@electron.princeton.edu

ground-state studies of many-particle systems have been conducted for pairwise additive potentials [1,4,6–11]. Often the ground states of short-range pairwise interactions are crystal structures in low dimensions [1,4,6–10,12], but long-range interactions exist that can suppress any kind of symmetry leading to disordered ground states in low dimensions [13,14]. Moreover, in sufficiently high dimensions, it has been suggested that even short-ranged pairwise interactions possess disordered ground states [15–17].

Ground states of purely repulsive pair interactions have profound connections not only to low-temperature states of matter but also to problems in pure mathematics, including discrete geometry and number theory [10,18,19], information theory, and computer science. As will be explained further below, it is known that the sphere-packing problem and the number-variance problem (closely related to an optimization problem in number theory) can be posed as energy minimizations associated with an infinite number of point particles in d-dimensional Euclidean space $\mathbb{R}^d$ interacting via certain repulsive pair potentials. Both of these problems can be interpreted to be optimization problems involving *point processes*, which can then be recast as energy minimizations. A point process in $\mathbb{R}^d$ is a distribution of an infinite number of points in $\mathbb{R}^d$ at number density ρ (number of points per unit volume) with configuration $\mathbf{r}_1, \mathbf{r}_2, \ldots$; see Ref. [16] for a precise mathematical definition.

A packing of congruent nonoverlapping spheres is a special point process in which there is a minimal pair separation distance, equal to the sphere diameter. The sphere-packing problem seeks to determine the densest arrangement(s) of congruent nonoverlapping d-dimensional spheres in Euclidean space $\mathbb{R}^d$ [18,20]. Although it is simple to state, it is a notoriously difficult problem to solve rigorously. Indeed, Kepler's four-century-old conjecture, which states that the face-centered-cubic (fcc) lattice in $\mathbb{R}^3$ is maximally dense, was only recently proved [21]. For $d \geq 4$, the packing problem remains unsolved [18,20,22]. It is well known that the sphere-packing problem can be posed as an energy minimization problem involving pairwise interactions between points in $\mathbb{R}^d$ (e.g., inverse power-law functions in which the exponent tends to infinity); see Ref. [10] and references therein.

Problems concerning the properties and quantification of density fluctuations in many-particle systems continue to provide many theoretical challenges. Of particular interest are density fluctuations that occur on some local length scale [23]. It has been shown that the minimal number variance associated with points (e.g., centroids of atomic or molecular systems) contained within some "window" can also be formulated as a ground-state problem involving bounded repulsive pair interactions with compact support [23,24]. For spherical windows in the large-radius limit, the best known solutions in $\mathbb{R}^d$ are usually point configurations that are duals (in the sense discussed later in the paper) to the best known sphere packings in $\mathbb{R}^d$.

The focus of this paper is on two other optimization problems involving point processes in $\mathbb{R}^d$: the *covering* and *quantizer* problems. Roughly speaking, the covering problem asks for the point configuration that minimizes the radius of overlapping spheres circumscribed around each of the points required to cover $\mathbb{R}^d$. The covering problem has applications in wireless communication network layouts [25], the search of high-dimensional data parameter spaces (e.g., search templates for gravitational waves) [26], and stereotactic radiation therapy [27]. The quantizer problem is concerned with finding the point configuration in $\mathbb{R}^d$ that minimizes a "distance error" associated with a randomly placed point and the nearest point of the point process. It has applications in computer science (e.g., data compression) [18], digital communications [18], coding and cryptography [28], and optimal meshing of space for numerical applications (e.g., quadrature and discretizing partial differential equations) [29]. Heretofore, the covering and quantizers problems were not known to correspond to any ground-state problems.

We reformulate the covering and quantizer problems as the determination of the ground states of interacting particles in $\mathbb{R}^d$ that generally involve single-body, two-body, three-body, and higher-body interactions. This is done by linking the covering and quantizer problems to certain optimization problems involving the void nearest-neighbor functions that arise in the theory of random media and statistical mechanics [2,30,31]. These reformulations, which again exemplify the deep interplay between geometry and physics, enable one to employ theoretical and numerical optimization techniques to solve these energy minimization problems. We find that disordered *saturated* sphere packings (roughly, packings in which no space exists to add an additional sphere) provide relatively thin (i.e., economical) coverings and may yield thinner coverings than the best known lattice coverings in sufficiently large dimensions. In the case of the quantizer problem, we derive improved upper bounds on the quantizer error that utilize sphere-packing solutions. These improved bounds are generally substantially sharper than an existing upper bound in low to moderately large dimensions. We also demonstrate that disordered saturated sphere packings yield relatively good quantizers. Our reformulation helps to explain why the known solutions of quantizer and covering problems are identical in the first three space dimensions and why they can be different for $d \geq 4$. In the first three space dimensions, the best known solutions of the sphere-packing and number-variance problems are directly related to those of the covering and quantizer problems, but such relationships may or may not exist for $d \geq 4$, depending on the peculiarities of the dimensions involved.

We begin by summarizing basic definitions and concepts in Sec. II. Because of the connections between the sphere-packing, number-variance, covering, and quantizer problems, in Sec. III, we formally define each of these problems, summarize key developments, and compare the best known solutions for each of them in selected dimensions. This includes calculations obtained in the present study for the best known number-variance solutions for $d=12$, 16, and 24. We then define in Sec. IV the void nearest-neighbor functions and represent them in terms of series involving certain integrals over the n-particle correlation functions, which statistically characterize an ensemble of interacting points. The special case of a single realization of the point distribution follows from this ensemble formulation, which reveals that the quantizer and covering problems can be expressed as ground-state solutions of many-body interactions of the gen-

eral form (1). Section V specifically gives these ground-state reformulations and shows how some known solutions in low dimensions can be explicitly recovered using the void nearest-neighbor functions. In Sec. VI, we show that *disordered* saturated sphere packings provide relatively thin coverings and may yield thinner coverings than the best known lattice coverings in sufficiently large dimensions. In Sec. VII, we derive improved upper bounds on the quantizer error that utilize sphere-packing solutions. We also show that *disordered* saturated sphere packings yield relatively good quantizers. Finally, in Sec. VIII, we make concluding remarks and comment on the application of the quantizer problem to the search for gravitational waves.

II. DEFINITIONS AND PRELIMINARIES

For a statistically homogeneous point process in $\mathbb{R}^d$ at number density ρ (number of points per unit volume), the quantity $\rho^n g_n(\mathbf{r}_1,\mathbf{r}_2,\ldots,\mathbf{r}_n)$ is proportional to the probability density for simultaneously finding n sphere centers at locations $\mathbf{r}_1,\mathbf{r}_2,\ldots,\mathbf{r}_n$ in $\mathbb{R}^d$ [1]. With this convention, each *n-particle correlation function* g_n approaches unity when all of the points become widely separated from one another. Statistical homogeneity implies that g_n is translationally invariant and therefore only depends on the relative displacements of the positions with respect to some arbitrarily chosen origin of the system, i.e.,

$$g_n = g_n(\mathbf{r}_{12},\mathbf{r}_{13},\ldots,\mathbf{r}_{1n}), \tag{3}$$

where $\mathbf{r}_{ij}=\mathbf{r}_j-\mathbf{r}_i$. As we will see, statistically homogeneous point processes include as special cases periodic point distributions.

The *pair-correlation* function $g_2(\mathbf{r})$ is a particularly important quantity. If the point process is also rotationally invariant (statistically isotropic), then g_2 depends on the radial distance $r\equiv|\mathbf{r}|$ only, i.e., $g_2(\mathbf{r})=g_2(r)$. Thus, it follows that the expected number of points $Z(R)$ found in a sphere of radius R from a randomly chosen point of the point process, called the *cumulative coordination function*, is given by

$$Z(R) = \rho\int_0^R s_1(r)g_2(r)dr, \tag{4}$$

where

$$s_1(r) = \frac{2\pi^{d/2}r^{d-1}}{\Gamma(d/2)} \tag{5}$$

is the surface area of a d-dimensional sphere of radius r.

A *lattice* Λ in $\mathbb{R}^d$ is a subgroup consisting of the integer linear combinations of vectors that constitute a basis for $\mathbb{R}^d$ and thus represents a special subset of point processes. In a lattice Λ, the space $\mathbb{R}^d$ can be geometrically divided into identical regions F called *fundamental cells*, each of which contains the just one point specified by the *lattice vector*

$$\mathbf{p} = n_1\mathbf{a}_1 + n_2\mathbf{a}_2 + \cdots + n_{d-1}\mathbf{a}_{d-1} + n_d\mathbf{a}_d, \tag{6}$$

where $\mathbf{a}_i$ are the basis vectors for the fundamental cell and n_i spans all the integers for $i=1,2,\ldots,d$. We denote by v_F the volume of the fundamental cell. In the physical sciences, a lattice is equivalent to a Bravais lattice. Unless otherwise stated, we will use the term lattice. Every lattice has a dual (or reciprocal) lattice Λ^* in which the sites of the lattice are specified by the dual (reciprocal) lattice vector $\mathbf{q}\cdot\mathbf{p}=2\pi m$, where $m=\pm1,\pm2,\pm3,\ldots$. The dual fundamental cell F^* has volume $v_{F^*}=(2\pi)^d/v_F$. This implies that the number density ρ of Λ is related to the number density ρ_* of the dual lattice Λ^* via the expression $\rho\rho_*=1/(2\pi)^d$. A *periodic* point process is a more general notion than a lattice because it is obtained by placing a fixed configuration of N points (where $N\geq1$) within one fundamental cell of a lattice Λ, which is then periodically replicated. Thus, the point process is still periodic under translations by Λ, but the N points can occur anywhere in the chosen fundamental cell.

Common d-dimensional lattices include the *hypercubic* $\mathbb{Z}^d$, *checkerboard* D_d, and *root* A_d lattices defined, respectively, by

$$\mathbb{Z}^d = \{(x_1,\ldots,x_d): x_i\in Z\},\quad d\geq1, \tag{7}$$

$$D_d = \{(x_1,\ldots,x_d)\in\mathbb{Z}^d: x_1+\cdots+x_d \text{ even}\},\quad d\geq3, \tag{8}$$

$$A_d = \{(x_0,x_1,\ldots,x_d)\in\mathbb{Z}^{d+1}: x_0+x_1+\cdots+x_d=0\},\quad d\geq1, \tag{9}$$

where $\mathbb{Z}$ is the set of integers $(\ldots,-3,-2,-1,0,1,2,3,\ldots)$; $x_1,\ldots,x_d$ denote the components of a lattice vector of either $\mathbb{Z}^d$ or D_d; and $x_0,x_1,\ldots,x_d$ denote a lattice vector of A_d. The d-dimensional lattices $\mathbb{Z}^d_*$, D^*_d, and A^*_d are the corresponding dual lattices; see Ref. [18] for definitions. The dual lattice $\mathbb{Z}^d_*$ is also a hypercubic lattice (even if the lattice spacing is 2π times the lattice spacing of $\mathbb{Z}^d$), and hence we say that the hypercubic lattice $\mathbb{Z}^d$ is equivalent (similar) to its dual lattice $\mathbb{Z}^d_*$, i.e., $\mathbb{Z}^d\equiv\mathbb{Z}^d_*$. Following Conway and Sloane [18], we say that two lattices are *equivalent* or *similar* if one becomes identical to the other by possibly rotation, reflection, and change of scale, for which we use the symbol $\equiv$. In fact, the hypercubic lattice $\mathbb{Z}^d$ is characterized by the stronger property of *self-duality*. A *self-dual* lattice is one with an *identical* dual lattice at density $\rho=\rho_*=1/(2\pi)^{d/2}$, i.e., without any rotation, reflection, or change of scale [32]. The A_d and D_d lattices can be regarded to be d-dimensional generalizations of the fcc lattice because this three-dimensional lattice is defined by $A_3\equiv D_3$. In one dimension, $A_1=A^*_1$ (equality meaning self-duality) is identical to the integer lattice $\mathbb{Z}^1=\mathbb{Z}$. In two dimensions, $A_2\equiv A^*_2$ defines the triangular lattice. In three dimensions, $A^*_3\equiv D^*_3$ defines the body-centered-cubic (bcc) lattice. The d-dimensional laminated lattice Λ_d [18,33] is of special interest. In dimensions 8 and 24, $\Lambda_8\equiv E_8$, where E_8 is the self-dual root lattice, and Λ_{24}, the self-dual Leech lattice, are remarkably symmetric and believed to be the densest sphere packings in those dimensions [22]. Thus, $E_8=E^*_8$ and $\Lambda_{24}=\Lambda^*_{24}$. The laminated lattice Λ_{16}, called the Barnes-Wall lattice, and the Coxeter-Todd lattice K_{12} are thought to be the densest lattice packings in 16 and 12 dimensions, respectively.

Note that for a single periodic point configuration at number density ρ, the radial pair-correlation function can be written as

$$g_2(r) = \sum_{i=1}^{\infty} \frac{Z_i}{\rho s_1(r_i)} \delta(r - r_i), \tag{10}$$

where Z_i is the coordination number at radial distance r_i (number of points that are exactly at a distance $r=r_i$ from a point of the point process) such that $r_{i+1} > r_i$ and $\delta(r)$ is a radial Dirac delta function. For cases in which each point is equivalent to any other, which includes all lattices and some periodic point processes, the coordination numbers Z_i are integers. For point processes for which the points are generally inequivalent, Z_i should be interpreted as the *expected* coordination number and hence will generally be a noninteger. Substitution of Eq. (10) into Eq. (4) gives the coordination function for such a periodic configuration as

$$Z(R) = \sum_{i=1}^{M} Z_i, \tag{11}$$

where M is the smallest integer for which $r_{M+1} > R$.

Consider any discrete set of points with position vectors $Y=\{\mathbf{r}_1, \mathbf{r}_2, \ldots\}$ in $\mathbb{R}^d$. Associated with each point $\mathbf{r}_i \in Y$ is its *Voronoi cell*, $\mathcal{V}(\mathbf{r}_i)$, which is defined to be the region of space nearer to the point at $\mathbf{r}_i$ than to any other point $\mathbf{r}_j$ in the set, i.e.,

$$\mathcal{V}(\mathbf{r}_i) = \{\mathbf{x}: |\mathbf{x} - \mathbf{r}_i| \leq |\mathbf{x} - \mathbf{r}_j| \text{ for all } \mathbf{r}_j \in Y\}. \tag{12}$$

The Voronoi cells are convex polyhedra whose interiors are disjoint, but share common faces, and therefore the union of all of the polyhedra is the whole of $\mathbb{R}^d$. This partition of space is called the *Voronoi* tessellation. The vertices of the Voronoi polyhedra are the points whose distance from the points Y is a local maximum. While the Voronoi polyhedra of a lattice are congruent to one another, the Voronoi polyhedra of a non-Bravais lattice are not identical to one another. A hole in a lattice is a point in $\mathbb{R}^d$ whose distance to the nearest lattice point is a local maximum. A *deep* hole is the one whose distance to a lattice point is a global maximum. The distance $\mathcal{R}_c$ to the deepest hole of a lattice is the *covering radius* and is equal to the *circumradius* of the associated Voronoi cell (the radius of the smallest circumscribed sphere).

In the case of the d-dimensional simple-cubic (hypercubic) lattice $\mathbb{Z}^d$, the Voronoi cell is a hypercube, and there is only one type of hole with covering radius $\mathcal{R}_c = \sqrt{d}/2$, assuming unit number density $\rho=1$. Figure 1 shows the Voronoi cell in the case $d=3$ as well as the corresponding Voronoi cells for the three-dimensional body-centered-cubic and face-centered-cubic lattices. Note that the truncated octahedron is the most spherically symmetric of the three Voronoi cells shown in Fig. 1 [34].

A sphere packing P in d-dimensional Euclidean space $\mathbb{R}^d$ is a collection of d-dimensional nonoverlapping congruent spheres. The *packing density* or, simply, density $\phi(P)$ of a sphere packing is the fraction of space $\mathbb{R}^d$ covered by the spheres. For spheres of diameter D and number density ρ, the density is given by

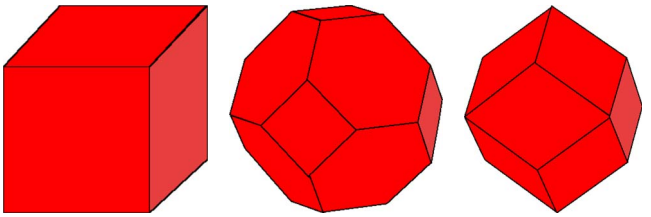

FIG. 1. (Color online) Voronoi cells in $\mathbb{R}^3$ for simple-cubic, body-centered-cubic, and face-centered-cubic lattices are the cube (left), truncated octahedron (middle), and rhombic dodecahedron (right), as adapted from Ref. [2]. The truncated octahedron is composed of six square and eight regular hexagonal faces. The rhombic dodecahedron is composed of 12 rhombus-shaped faces.

$$\phi = \rho v_1(D/2), \tag{13}$$

where

$$v_1(R) = \frac{\pi^{d/2}}{\Gamma(1 + d/2)} R^d \tag{14}$$

is the volume of a d-dimensional sphere of radius R.

A packing is saturated if there is no space available to add another sphere without overlapping the existing particles. We denote the packing density of such a packing by ϕ_s. A *lattice packing* P_L is the one in which the centers of nonoverlapping spheres are located at the points of Λ. Thus, the density of a lattice packing ϕ^L consisting of spheres of diameter D is given by

$$\phi^L = \frac{v_1(D/2)}{v_F}, \tag{15}$$

where v_F is the volume of a fundamental cell. A periodic packing of congruent spheres is obtained by placing a fixed configuration of N sphere centers (where $N \geq 1$) within one fundamental cell of a lattice Λ, which is then periodically replicated without overlaps. The packing density of a periodic packing is given by

$$\phi = \frac{N v_1(D/2)}{v_F} = \rho v_1(D/2), \tag{16}$$

where $\rho = N/v_F$ is the number density.

III. PROBLEM STATEMENTS AND BACKGROUND

A. Sphere-packing problem

The sphere-packing problem seeks to answer the following question: among all packings of congruent spheres, what is the maximal packing density ϕ_{max}, i.e., largest fraction of $\mathbb{R}^d$ covered by the spheres, and what are the corresponding arrangements of the spheres [18,35]? More precisely, the maximal density is defined by

$$\phi_{max} = \sup_{P \subset \mathbb{R}^d} \phi(P), \tag{17}$$

where the supremum is taken over all packings in $\mathbb{R}^d$. The sphere-packing problem is of great fundamental and practical

TABLE I. Best known solutions to the sphere-packing problem in selected dimensions; see Conway and Sloane [18] for details.

Dimension d	Packing	Packing density ϕ
1	$A_1^*=\mathbb{Z}$	1
2	$A_2^*\equiv A_2$	$\pi/\sqrt{12}=0.906899\ldots$
3	$A_3\equiv D_3$	$\pi/\sqrt{18}=0.740480\ldots$
4	$D_4\equiv D_4^*$	$\pi^2/16=0.616850\ldots$
5	D_5	$2\pi^2/(30\sqrt{2})=0.465257\ldots$
6	E_6	$3\pi^3/(144\sqrt{3})=0.372947\ldots$
7	E_7	$\pi^3/105=0.295297\ldots$
8	$E_8=E_8^*$	$\pi^4/384=0.253669\ldots$
9	Λ_9	$\sqrt{2}\pi^4/945=0.145774\ldots$
10	P_{10c}	$\pi^5/3072=0.099615\ldots$
12	Λ_{12}^{max}	$\pi^6/23040=0.041726\ldots$
16	Λ_{16}	$\pi^8/645120=0.014708\ldots$
24	$\Lambda_{24}=\Lambda_{24}^*$	$\pi^{24}/479001600=0.001929\ldots$

interest and arises in a variety of contexts, including classical ground states of matter in low dimensions [6], the famous Kepler conjecture for $d=3$ [21], error-correcting codes [18,36], and spherical codes [18].

The optimal solutions are known only for the first three space dimensions [21]. For $4\leq d\leq 9$, the densest known packings are Bravais lattice packings [18]. For example, the checkerboard lattice D_d, which is the d-dimensional generalization of the fcc lattice (densest packing in $\mathbb{R}^3$), is believed to be optimal in $\mathbb{R}^4$ and $\mathbb{R}^5$. The remarkably symmetric self-dual E_8 and Leech lattices in $\mathbb{R}^8$ and $\mathbb{R}^{24}$, respectively, are most likely the densest packings in these dimensions [22]. Table I summarizes the densest known packings in selected dimensions.

For large d, the best that one can do theoretically is to devise upper and lower bounds on ϕ_{max} [16,18,20]. For example, Minkowski [37] proved that the maximal density ϕ_{max}^L among all Bravais lattice packings for $d\geq 2$ satisfies the lower bound

$$\phi_{max}^L \geq \frac{\zeta(d)}{2^{d-1}}, \tag{18}$$

where $\zeta(d)=\Sigma_{k=1}^{\infty}k^{-d}$ is the Riemann zeta function. It is seen that for large values of d, the asymptotic behavior of the *nonconstructive* Minkowski lower bound is controlled by 2^{-d}. Note that the density of a saturated packing of congruent spheres in $\mathbb{R}^d$ for all d satisfies

$$\phi \geq \frac{1}{2^d}, \tag{19}$$

which has the same dominant exponential term as Eq. (18). This is a rather weak lower bound on the density of saturated packings because there exists a disordered but *unsaturated packing construction* in $\mathbb{R}^d$, known as the "ghost" random sequential addition (RSA) packing [15], which achieves the density 2^{-d} in any dimension. We will employ these results in Sec. VII B. It is also known that there are saturated packings in $\mathbb{R}^d$ with densities that exceed the scaling 2^{-d} [38], as we will discuss in Sec. III C. In the large-dimensional limit, Kabatiansky and Levenshtein [39] showed that the maximal density is bounded from above according to the asymptotic upper bound

$$\phi_{max} \leq \frac{1}{2^{0.5990d}}. \tag{20}$$

We will employ sphere-packing solutions to obtain heretofore unattained results for both the covering and quantizer problems. In particular, we obtain coverings and quantizers utilizing disordered saturated packings in Secs. VI and VII C, respectively. In Sec. VII, we use the densest lattice packings to derive improved upper bounds on the quantizer error.

B. Number-variance problem, hyperuniformity, and Epstein zeta function

We denote by $\sigma^2(A)$ the variance in the number of points $N(A)$ contained within a window $A\subset\mathbb{R}^d$. The number variance $\sigma^2(A)$ for a specific choice of A is necessarily a positive number and is generally related to the *total correlation function* $h(\mathbf{r})=g_2(\mathbf{r})-1$ for a translationally invariant point process [23], where g_2 is the pair-correlation function defined in Sec. II. In the special case of a spherical window of radius R in $\mathbb{R}^d$, the number variance is explicitly given by

$$\sigma^2(R) = \rho v_1(R)\left[1+\rho\int_{\mathbb{R}^d} h(\mathbf{r})\alpha(r;R)d\mathbf{r}\right], \tag{21}$$

where $\alpha(r;R)$ is the dimensionless volume common to two spherical windows of radius R [in units of the volume of a spherical window of radius R, $v_1(R)$] whose centers are separated by a distance r. We will call $\alpha(r;R)$ the *scaled intersection volume*, which will play an important role in this paper. The scaled intersection volume has the support $[0,2R]$, the range $[0,1]$, and the following alternative integral representation [16]:

$$\alpha(r;R) = c(d)\int_0^{\cos^{-1}[r/(2R)]}\sin^d(\theta)d\theta, \tag{22}$$

where $c(d)$ is the d-dimensional constant given by

$$c(d) = \frac{2\Gamma(1+d/2)}{\pi^{1/2}\Gamma[(d+1)/2]}. \tag{23}$$

Torquato and Stillinger [16] found the following series representation of the scaled intersection volume $\alpha(r;R)$ for $r\leq 2R$ and for any d:

$$\alpha(r;R) = 1-c(d)x+c(d)\sum_{n=2}^{\infty}(-1)^n \times\frac{(d-1)(d-3)\cdots(d-2n+3)}{(2n-1)[2\times 4\times 6\cdots(2n-2)]}x^{2n-1}, \tag{24}$$

where $x=r/(2R)$. For even dimensions, relation (24) is an infinite series because it involves transcendental functions;

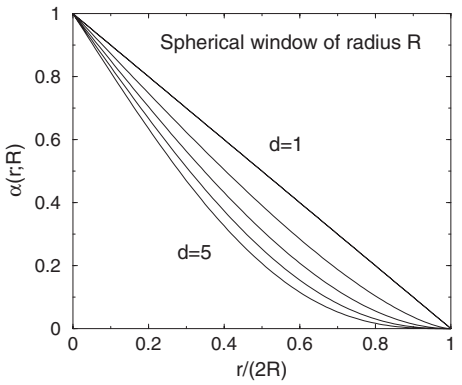

FIG. 2. The scaled intersection volume $\alpha(r;R)$ for spherical windows of radius R as a function of r for the first five space dimensions. The uppermost curve is for $d=1$ and lowermost curve is for $d=5$.

but for odd dimensions, the series truncates such that $\alpha(r;R)$ is a uninvariate polynomial of degree d. For example, in two and three dimensions, respectively, the scaled intersection volumes are given by

$$\alpha(r;R) = \frac{2}{\pi}\left[\cos^{-1}\left(\frac{r}{2R}\right) - \frac{r}{2R}\left(1-\frac{r^2}{4R^2}\right)^{1/2}\right]\Theta(2R-r) \quad (d=2), \tag{25}$$

$$\alpha(r;R) = \left[1 - \frac{3}{4}\frac{r}{R} + \frac{1}{16}\left(\frac{r}{R}\right)^3\right]\Theta(2R-r) \quad (d=3), \tag{26}$$

where

$$\Theta(x) = \begin{cases} 0, & x<0 \\ 1, & x\geq 0 \end{cases} \tag{27}$$

is the Heaviside step function. Figure 2 provides plots of $\alpha(r;R)$ as a function of r for the first five space dimensions. For any dimension, $\alpha(r;R)$ is a monotonically decreasing function of r. At a fixed value of r in the interval $(0,2R)$, $\alpha(r;R)$ is a monotonically decreasing function of the dimension d.

For large R, it has been proved that $\sigma^2(R)$ cannot grow more slowly than γR^{d-1}, where γ is a positive constant [40]. We note that point processes (translationally invariant or not) for which $\sigma^2(R)$ grows more slowly than the window volume (i.e., as R^d) for large R are examples of *hyperuniform* (or superhomogeneous) point patterns [23]. For hyperuniform point processes in which the number variance grows like the surface area of the window, one has

$$\sigma^2(R) = 2^d\eta\left[B\left(\frac{R}{\mathcal{D}}\right)^{d-1} + \mathcal{O}\left(\frac{R}{\mathcal{D}}\right)^{d-2}\right], \quad R\to\infty, \tag{28}$$

where

$$B = \frac{\eta c(d)}{2\mathcal{D}v_1(\mathcal{D}/2)}\int_{\mathbb{R}^d} h(\mathbf{r})r\,d\mathbf{r} \tag{29}$$

is a dimensionless constant with $c(d)$ defined by Eq. (23),

$$\eta = \rho v_1(\mathcal{D}/2) \tag{30}$$

is a dimensionless density, and $\mathcal{D}$ represents some "microscopic" length scale, such as the minimum pair separation distance in a packing or the mean nearest-neighbor distance. This class of hyperuniform point processes includes all periodic point patterns, quasicrystals that possess Bragg peaks, and disordered hyperuniform point patterns in which the pair-correlation functions decay exponentially fast to unity [23].

It has been shown that finding the point process that minimizes the number variance $\sigma^2(R)$ is equivalent to finding the ground state of a certain repulsive pair potential with compact support [23]. Specifically, by invoking a volume-average interpretation of the number-variance problem valid for a single realization of a point process, Torquato and Stillinger found [23]

$$\sigma^2(R) = 2^d\eta B_N(R)\left(\frac{R}{\mathcal{D}}\right)^{d-1}, \tag{31}$$

where

$$B_N(R) = \frac{R}{\mathcal{D}}\left[1 - 2^d\eta\left(\frac{R}{\mathcal{D}}\right)^d + \frac{1}{N}\sum_{i\neq j}^{N}\alpha(r_{ij};R)\right]. \tag{32}$$

The asymptotic coefficient B defined by Eq. (29) for a hyperuniform point pattern is then related to $B_N(R)$ by the expression

$$B = \lim_{L\to+\infty}\frac{1}{L}\int_0^L B_N(R)dR. \tag{33}$$

These results imply that the asymptotic coefficient B obtained in Eq. (29) involves an average over small-scale fluctuations in the number variance with length scale on the order of the mean separation between points [23]. In the special case of a (Bravais) lattice Λ, one can express the rescaled surface-area coefficient as follows:

$$\eta^{1/d}B = \frac{\pi^{(d-1)/2}2^{d-1}[\Gamma(1+d/2)]^{1-1/d}}{v_F^{1+1/d}}\sum_{\mathbf{q}\neq\mathbf{0}}\frac{1}{\|\mathbf{q}\|^{d+1}}, \tag{34}$$

where we recall that v_F is the volume of the fundamental cell of the lattice Λ and $\mathbf{q}$ represents a lattice vector in the dual (or reciprocal) lattice Λ^*. The rescaled coefficient $\eta^{1/d}B$ renders the result independent of the length scale in the lattice [23].

Finding the lattice that minimizes B is directly related to an outstanding problem in number theory, namely, finding the minima of the Epstein zeta function $Z_\Lambda(s)$ [19] defined by

$$Z_\Lambda(s) = \sum_{\mathbf{p}\neq\mathbf{0}}\frac{1}{\|\mathbf{p}\|^{2s}}, \tag{35}$$

where $\mathbf{p}$ is a lattice vector of the lattice Λ. Note that the dual of the lattice that minimizes the Epstein zeta function at $s=(d+1)/2$ among all lattices will minimize the scaled asymptotic number-variance coefficient (34) among lattices [23,41]. Certain duality relations have been derived that establish rigorous upper bounds on the energies of such ground

TABLE II. Best known solutions to the asymptotic number-variance problem in selected dimensions. Values reported for $d=1$, 2, and 3 and $d=4-8$ are taken from Torquato and Stillinger [23] and Zachary and Torquato [41], respectively. Values reported for $d=12$, 16, and 24 have been determined in the present work.

Dimension d	Structure	Scaled coefficient $\eta^{1/d}B$
1	$A_1^*=\mathbb{Z}$	0.083333
2	$A_2^*\equiv A_2$	0.12709
3	$A_3^*\equiv D_3^*$	0.15560
4	$D_4^*\equiv D_4$	0.17488
5	Λ_5^{2*}	0.19069
6	E_6^*	0.20221
7	D_7^+	0.21037
8	$E_8^*=E_8=D_8^+$	0.21746
12	$K_{12}^*\equiv K_{12}$	0.24344
16	$\Lambda_{16}^*\equiv\Lambda_{16}$	0.25629
24	$\Lambda_{24}^*=\Lambda_{24}$	0.26775

states and help to identify energy-minimizing lattices [5]. Because $Z_\Lambda(s)$ is globally minimized for $d=1$ by the integer lattice [23] and is minimized for $d=2$ among all lattices by the triangular lattice [42], it has been conjectured that the Epstein zeta function for $s>0$ is minimized among lattices by the maximally dense lattice packing for any dimension d [43,44]. Sarnak and Strömbergsson [19] proved that the conjecture cannot be generally true; but for $d=4$, 8, and 24, the densest lattice packing is a strict local minimum. Since as $s\to+\infty$ the minimizer of Epstein zeta function is the densest sphere packing in $\mathbb{R}^d$ for any d, it is likely that in the high-dimensional limit the minimizers of this function are nonlattices, namely, disordered sphere packings [16].

In Table II, we tabulate the best known solutions to the asymptotic number-variance problem in selected dimensions. Values for the first three space dimensions were given in Ref. [23] and those for $d=4-8$ were provided in Ref. [41]. The values reported for $d=12$, 16, and 24 were ascertained using efficient algorithms based on alternative number-theoretic representations of the Epstein zeta function $Z_\Lambda(s)$ [19] for the corresponding densest known lattice packings for $s=(d+1)/2$ and then using the duality relations connecting it to the asymptotic surface-area coefficient for the number variance. Appendix A provides details for these computations.

C. Covering problem

Surround each of the points of a point process $\mathcal{P}$ in $\mathbb{R}^d$ by congruent overlapping spheres of radius R such that the spheres cover the space. The *covering density* θ is defined as follows:

$$\theta=\rho v_1(R), \tag{36}$$

where $v_1(R)$ is given by Eq. (14). The *covering problem* asks for the arrangement of points with the least density θ. We define the covering radius $\mathcal{R}_c$ for any configuration of points in $\mathbb{R}^d$ to be the minimal radius of the overlapping spheres to cover $\mathbb{R}^d$. Figure 3 shows two examples of coverings in the plane.

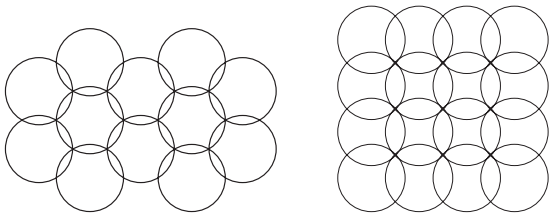

FIG. 3. Coverings of the plane with overlapping circles centered on the triangular lattice (left panel) and the square lattice (right panel). The triangular lattice $A_2\equiv A_2^*$ provides the best covering among all point processes at unit number density $\rho=1$ with $\theta=2\pi/(3\sqrt{3})=1.2092\ldots$ [18]. This is to be compared to the square lattice $\mathbb{Z}^2$ with $\theta=\pi/2=1.5708\ldots$.

The covering density associated with A_d^* at unit number density $\rho=1$ is known exactly for any dimension d [18]:

$$\theta=v_1(1)\sqrt{d+1}\left[\frac{d(d+2)}{12(d+1)}\right]^{d/2}. \tag{37}$$

For the hypercubic lattice $\mathbb{Z}^d$ at $\rho=1$,

$$\theta=v_1(1)\frac{d^{d/2}}{2^d}. \tag{38}$$

Thus, the ratio of the covering density for A_d^* to that of $\mathbb{Z}^d$ is given by

$$\frac{\theta(A_d^*)}{\theta(Z^d)}=\frac{\sqrt{d+1}}{3^{d/2}}\left[\frac{d+2}{d+1}\right]^{d/2}. \tag{39}$$

For large d, this ratio becomes

$$\frac{\theta(A_d^*)}{\theta(Z^d)}\sim\frac{\sqrt{de}}{3^{d/2}}, \tag{40}$$

and thus we see that A_d^* provides exponentially thinner coverings than that of $\mathbb{Z}^d$ in the large-d limit. We note that in this asymptotic limit,

$$\theta(A_d^*)\sim\left(\frac{e}{\pi}\right)^{1/2}\left(\frac{e\pi}{6}\right)^{1/2}$$
$$=0.865\,255\,979\,2\ldots(1.193\,016\,780\ldots)^d. \tag{41}$$

Until recently, A_d^* was the best known lattice covering in all dimensions $d\leq 23$. However, for most dimensions in the range $6\leq\theta\leq 15$, Schürmann and Vallentin [45] discovered other lattice coverings that are slightly thinner than those for A_d^*. Table III provides the best known solutions to the covering problem in selected dimensions.

Until the present work, there were no known explicit nonlattice constructions possessing covering densities smaller than those of the best lattice coverings in any dimension d [18]. In Sec. VII, we provide evidence that certain disordered point patterns give thinner coverings than the best known lattice coverings beginning at $d=17$. There is a fundamental difference between coverings associated with point patterns that have identical Voronoi cells (i.e., lattices and periodic

TABLE III. Best known solutions to the covering problem in selected dimensions. Values reported are taken from Conway and Sloane [18], except for $d=7$, 8, and 9, which were obtained from Schürmann and Vallentin [45]. It is only in one and two dimensions that these solutions have been proved to be globally optimal [18].

Dimension d	Covering	Covering density θ
1	$A_1^*=\mathbb{Z}$	1
2	$A_2^*\equiv A_2$	1.2092
3	$A_3^*\equiv D_3^*$	1.4635
4	A_4^*	1.7655
5	A_5^*	2.1243
6	L_6^{c1}	2.4648
7	L_7^c	2.9000
8	L_8^c	3.1422
9	A_9^5	4.3401
10	A_{10}^*	5.2517
12	A_{12}^*	7.5101
16	A_{16}^*	15.3109
17	A_{17}^*	18.2878
18	A_{18}^*	21.8409
24	$\Lambda_{24}=\Lambda_{24}^*$	7.9035

point patterns in which each point is equivalent) and those point processes whose Voronoi cells are generally different (e.g., irregular point processes). This salient point is illustrated in Fig. 4 and explained in the corresponding caption.

Rogers showed that (possibly nonlattice) coverings exist with

$$\theta \leq 5d + d\ln(d) + d\ln[\ln(d)], \tag{42}$$

for $d \geq 2$. This is a nonconstructive upper bound. This upper bound provides a substantially thinner covering density than that of the A_d^* lattice in the large-d limit [cf. Eq. (41)], but it is not known whether this bound becomes sharp in the large-d limit.

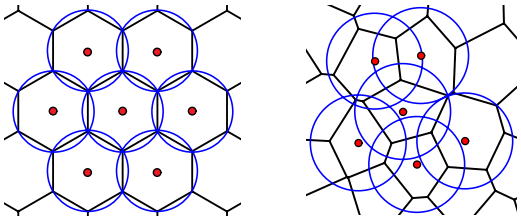

FIG. 4. (Color online) For lattices or periodic point process in which each point is equivalent, the Voronoi cells are congruent to one another, the Voronoi centroids coincide with the points of the point process, and the covering radius $\mathcal{R}_c$ is equal to the circumradius of the associated Voronoi cell. For an irregular point pattern, generally, the Voronoi cells are not congruent to one another, the Voronoi centroids do not coincide with the points of the point process, and the covering radius $\mathcal{R}_c$ is not equal to the circumradius of the associated Voronoi cell. These two instances are illustrated in two dimensions for the triangular lattice and an irregular point pattern.

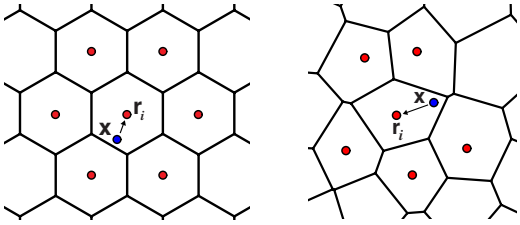

FIG. 5. (Color online) Examples of two-dimensional quantizers. Any point $\mathbf{x}$ is quantized ("rounded off") to the nearest point $\mathbf{r}_i$. Left panel: triangular lattice (best quantizer in $\mathbb{R}^2$ [18]). Right panel: irregular point process.

The best lower bound on the covering density is given by

$$\theta \geq \tau_d. \tag{43}$$

To define τ_d, let S be a regular simplex with edge length equal to 2. Spheres of radius $\sqrt{2d/(d+1)}$ centered at the vertices of S just cover S. The quantity τ_d is the ratio of the sums of the intersections of these spheres with S to the volume of S. Thus, in the large-d limit, $\tau \to d/e^{3/2}$.

D. Quantizer problem

Consider a point process $\mathcal{P}$ in $\mathbb{R}^d$ with configuration $\mathbf{r}_1, \mathbf{r}_2, \ldots, \mathbf{r}_N$. A d-dimensional quantizer is a device that takes as an input a point at position $\mathbf{x}$ in $\mathbb{R}^d$ generated from some probability density function $p(\mathbf{x})$ and outputs the nearest point $\mathbf{r}_i$ of the point process to $\mathbf{x}$. Equivalently, if the input $\mathbf{x}$ belongs to the Voronoi cell $\mathcal{V}(\mathbf{r}_i)$, the output is $\mathbf{r}_i$ (see Fig. 5). For simplicity, we assume that $\mathbf{x}$ is uniformly distributed over a large ball in $\mathbb{R}^d$ containing the N points of the point process. One attempts to choose the configuration $\mathbf{r}_1, \mathbf{r}_2, \ldots, \mathbf{r}_N$ of the point process to minimize the mean-squared error, i.e., the expected value of $|\mathbf{x}-\mathbf{r}_i|^2$. Specifically, the quantizer problem is to choose the N-point configuration so as to minimize the *scaled dimensionless error* (sometimes called the *distortion*) [18]

$$\mathcal{G} = \frac{1}{d}\langle R^2 \rangle, \tag{44}$$

where

$$\langle R^2 \rangle = \frac{\lim_{N\to\infty} \frac{1}{N} \sum_{i=1}^{N} \int_{\mathcal{V}(\mathbf{r}_i)} |\mathbf{x}-\mathbf{r}_i|^2 d\mathbf{x}}{\langle V(\mathcal{V}) \rangle^{1+2/d}} \tag{45}$$

is a dimensionless error and

$$\langle V(\mathcal{V}) \rangle = \left[\lim_{N\to\infty} \frac{1}{N} \sum_{i=1}^{N} V(\mathcal{V}(\mathbf{r}_i)) \right] \tag{46}$$

is the expected volume of a Voronoi cell, and $V(\mathcal{V}(\mathbf{r}_i))$ is the volume of the ith Voronoi cell. The scaling factor $1/d$ in (44) is included to compare the second moments appropriately across dimensions. We will denote the minimal scaled dimensionless error by $\mathcal{G}_{min}$. Note that since there is one point per Voronoi cell, the number density ρ is set equal to unity.

TABLE IV. Best known solutions to the quantizer problem in selected dimensions. Values reported are taken from Conway and Sloane [18], except for $d=9$ and 10, which were obtained from Agrell and Eriksson [47]. It is only in one and two dimensions that these solutions have been proved to be globally optimal [18].

Dimension d	Quantizer	Scaled error $\mathcal{G}$
1	$A_1^*=\mathbb{Z}$	0.083333
2	$A_2^*\equiv A_2$	0.080188
3	$A_3^*\equiv D_3^*$	0.078543
4	$D_4^*\equiv D_4$	0.076603
5	D_5^*	0.075625
6	E_6^*	0.074244
7	E_7^*	0.073116
8	$E_8^*=E_8$	0.071682
9	L_9^{AE}	0.071626
10	D_{10}^+	0.070814
12	$K_{12}^*\equiv K_{12}$	0.070100
16	$\Lambda_{16}^*\equiv\Lambda_{16}$	0.068299
24	$\Lambda_{24}^*=\Lambda_{24}$	0.065771

If all of the Voronoi cells are congruent (as they are in the case of all lattices and some periodic point processes), we have the simpler expression

$$\mathcal{G}=\frac{\frac{1}{d}\int_{\mathcal{V}}|\mathbf{x}|^2d\mathbf{x}}{V(\mathcal{V})^{1+2/d}}, \tag{47}$$

where the centroid of the Voronoi cell $\mathcal{V}$ is the origin of the coordinate system. The *lattice quantizer problem* is to find the lattice for which $\mathcal{G}$, given by Eq. (47), is minimum. Thus, $\mathcal{G}$ can be interpreted as the scaled dimensionless *second moment of inertia* of the Voronoi cell.

The best known quantizers in any dimension d are usually lattices that are the duals of the densest known packings (see the discussion in Sec. III A and Ref. [18]), except in dimensions 9 and 10, where the best solutions are still lattices, but are not duals of the densest lattice packings in those dimensions. Although the best known solutions of the quantizer and covering problems are the same in the first three space dimensions, they are generally different for $d\geq 4$ [18,45]. Zador [46] derived upper and lower bounds on $\mathcal{G}_{min}$. Conway and Sloane [18] obtained conjectural lower bounds on $\mathcal{G}_{min}$. We defer the discussion of these bounds to Sec. VII, where we derive sharper upper bounds on $\mathcal{G}_{min}$, among other results. Table IV provides the best known solutions to the quantizer problem in selected dimensions.

E. Comparison of the four problems

Table V lists the best known solutions of the quantizer, covering, and number-variance problems and sphere-packing problems in $\mathbb{R}^d$ for selected d. It is seen that in the first two space dimensions, the best known solutions for each of these four problems are identical to one another. For $d=3$, the densest sphere packing is the D_3 or, equivalently, A_3 lattice, which is the dual lattice associated with the best known solutions to the quantizer, covering, and number-variance problems, which is the A_3^* lattice. Thus, for the first three space dimensions, the best known solutions for each of the four problems are lattices, and they are either identical to one another or duals of one another. However, such relationships may or may not exist for $d\geq 4$, depending on the peculiarities of the dimensions involved.

TABLE V. Comparison of the best known solutions to the quantizer, covering, number-variance, and sphere-packing problems, as obtained from the previous four tables. Recall that the E_8 and Λ_{24} lattices are self-dual lattices.

Dimension d	Quantizer	Covering	Variance	Packing
1	$A_1^*=\mathbb{Z}$	$A_1^*=\mathbb{Z}$	$A_1^*=\mathbb{Z}$	$A_1^*=\mathbb{Z}$
2	$A_2^*\equiv A_2$	$A_2^*\equiv A_2$	$A_2^*\equiv A_2$	$A_2^*\equiv A_2$
3	$A_3^*\equiv D_3^*$	$A_3^*\equiv D_3^*$	$A_3^*\equiv D_3^*$	$A_3\equiv D_3$
4	$D_4^*\equiv D_4$	A_4^*	$D_4^*\equiv D_4$	$D_4^*\equiv D_4$
5	D_5^*	A_5^*	Λ_5^{2*}	D_5
6	E_6^*	L_6^{c1}	E_6^*	E_6
7	E_7^*	L_7^c	Λ_7^{3*}	E_7
8	E_8	L_8^c	E_8	E_8
9	L_9^{AE}	A_9^5	Λ_9^*	Λ_9
10	D_{10}^+	A_{10}^*	Λ_{10}^*	P_{10c}
12	K_{12}	A_{12}^*	Λ_{12}^{max*}	Λ_{12}^{max}
16	Λ_{16}^*	A_{16}^*	Λ_{16}^*	Λ_{16}
24	Λ_{24}	Λ_{24}	Λ_{24}	Λ_{24}

There is a fundamental difference between the nature of the interactions for the sphere-packing problem and those for the other three problems. Any sphere packing (optimal or not) consisting of nonoverlapping spheres of diameter D is described by a short-ranged pair potential that is zero whenever the spheres do not overlap (when the pair separation distance is greater than D) and is infinite whenever the pair separation distance is less than D. By contrast, the other three problems are described by "soft" bounded interactions. In particular, we have seen that the number variance is specified by a bounded repulsive pair potential with compact support [cf. Eq. (31)]. We will see in the subsequent sections that the covering and quantizer problems are described by many-particle bounded interactions but of the more general form (1), which involves single-body, two-body, three-body, and higher-body interactions.

One simple reason why the best known solutions of the sphere-packing and number-variance problems are related to one another either directly or via their dual solutions in the first three space dimensions is that they both involve short-ranged repulsive pair interactions only. The reader is referred to Refs. [5,23] for a comprehensive explanation. The reasons why the best known solutions to these two problems are sometimes the best known solutions for the covering and quantizer problems will become apparent in the subsequent sections. The explanation for why the best known covering and quantizer solutions are generally different for $d\geq 4$ is discussed in Sec. V. We note that the Leech lattice Λ_{24} for $d=24$ is an exceptional case in that it likely provides the

globally optimal solution to all four different problems. The remarkably high degree of symmetry possessed by this self-dual lattice [22] accounts for this unique property. The only other dimensions where all four solutions are the same and globally optimal are $d=1$ and $d=2$.

IV. NEAREST-NEIGHBOR FUNCTIONS

A. Definitions

We recall the definition of the void nearest-neighbor probability density function $H_V(R)$ [2]:

$$H_V(R)dR = \text{Probability that a point of the point process lies at a distance between } R \text{ and } R+dR \text{ from a randomly chosen point in } \mathbb{R}^d. \tag{48}$$

The void exclusion probability $E_V(R)$ is the *complementary cumulative distribution function* associated with $H_V(R)$:

$$E_V(R) = \int_R^\infty H_V(x)dx, \tag{49}$$

and hence is a monotonically decreasing function of R [2]. Thus, $E_V(R)$ has the following probabilistic interpretation:

$$E_V(R) = \text{Probability of finding a randomly placed spherical cavity of radius } R \text{ empty of any points.} \tag{50}$$

There is another interpretation of E_V that involves circumscribing spheres of radius R around each point in a realization of the point process. It immediately follows that $E_V(R)$ is the expected fraction of space not covered by these circumscribing spheres. Differentiating Eq. (49) with respect to R and multiplying by negative one gives

$$H_V(R) = -\frac{\partial E_V}{\partial R}. \tag{51}$$

Note that these void quantities are different from the "particle" nearest-neighbor functions [31,48,49] in which the sphere of radius R is centered at an actual point of the point process (as opposed to an arbitrary point in the space).

It is useful to introduce the "conditional" nearest-neighbor function $G_V(r)$ [30,31], which is defined in terms of $H_V(r)$ and $E_V(r)$ as follows:

$$H_V(R) = \rho s_1(R) G_V(R) E_V(R), \tag{52}$$

where $s_1(R)$ is the surface area of a d-dimensional sphere of radius R [cf. Eq. (5)]. Thus, we have the following interpretation of the conditional function:

$$\rho s_1(R) G_V(R)\, dR = \text{Given that a spherical cavity of radius } R \text{ centered at an arbitrary point in the space is empty of any points of the point process, the probability of finding a point in the spherical shell of volume } s_1(R)dR \text{ surrounding the arbitrary point.} \tag{53}$$

Therefore, it follows from Eqs. (51) and (52) that the exclusion probability can be expressed in terms of G_V via the relation

$$E_V(R) = \exp\left[-\rho s_1(1)\int_0^R x^{d-1} G_V(x)dx\right]. \tag{54}$$

It is clear that the void functions have the following behaviors at the origin for $d \geq 2$ [50]:

$$E_V(0) = 1, \quad H_V(0) = 0, \quad G_V(0) = 1. \tag{55}$$

Moments of the nearest-neighbor function $H_V(R)$ arise in rigorous bounds for transport properties of random media [2]. The nth moment of $H_V(R)$ is defined as

$$\langle R^n \rangle = \int_0^\infty R^n H_V(R)dR = n\int_0^\infty R^{n-1} E_V(R)dR. \tag{56}$$

B. Series representations

The void functions can be expressed as an infinite series whose terms are integrals over the n-particle density functions [2,31]. For example, the void exclusion probability functions for a translationally invariant point process are, respectively, given by

$$E_V(R) = 1 + \sum_{k=1}^{\infty} (-1)^k \frac{\rho^k}{k!} \int_{\mathbb{R}^d} g_k(\mathbf{r}_1, \ldots, \mathbf{r}_k) \times \prod_{j=1}^{k} \Theta(R - |\mathbf{x} - \mathbf{r}_j|) d\mathbf{r}_j, \tag{57}$$

where g_n is the n-particle correlation function and $\Theta(x)$ is the Heaviside step function defined by Eq. (27). The corresponding series for $H_V(R)$ is obtained from the series above using Eq. (51).

Note that the series (57) can be rewritten in terms of intersection volumes of spheres:

$$E_V(R) = 1 + \sum_{k=1}^{\infty} (-1)^k \frac{\rho^k}{k!} \int_{\mathbb{R}^d} g_k(\mathbf{r}_1, \ldots, \mathbf{r}_k) v_k^{\text{int}}(\mathbf{r}_1, \ldots, \mathbf{r}_k; R) \times d\mathbf{r}_1 \cdots d\mathbf{r}_k, \tag{58}$$

where

$$v_n^{\text{int}}(\mathbf{r}_1, \ldots, \mathbf{r}_n; R) = \int d\mathbf{x} \prod_{j=1}^{n} \Theta(R - |\mathbf{x} - \mathbf{r}_j|) \tag{59}$$

is the intersection volume of n equal spheres of radius R centered at positions $\mathbf{r}_1, \ldots, \mathbf{r}_n$. Observe that $v_2^{\text{int}}(r;R) = v_1(R)\alpha(r;R)$, where $v_1(R)$ is the volume of a sphere of radius R [cf. Eq. (14)] and $\alpha(r;R)$ is the scaled intersection volume [cf. Eqs. (22) and (24)].

In the special case of a Poisson point distribution, $g_n = 1$ for all n, and hence Eq. (58) immediately yields the well-known exact result for such a spatially uncorrelated point process,

$$E_V(R) = \exp[-\rho v_1(R)]. \tag{60}$$

The use of this relation with definition (51) gives

$$H_V(R) = \rho s_1(R) \exp[-\rho v_1(R)]. \tag{61}$$

For a single realization of N points within a large volume V in $\mathbb{R}^d$, we have

$$E_V(R) = 1 - \rho v_1(R) + \frac{1}{V} \sum_{i<j} v_2^{\text{int}}(r_{ij};R) - \frac{1}{V} \sum_{i<j<k} v_3^{\text{int}}(r_{ij}, r_{ik}, r_{jk}; R) + \cdots. \tag{62}$$

This formula assumes that N is sufficiently large, so that boundary effects can be neglected. The second term in Eq. (62), $\rho v_1(R) = \sum_{i=1}^{N} v_1(R)/V$, can be interpreted as a sum over one-body terms, which is independent of the point configuration. Clearly, the $(n+1)$th term in Eq. (62) can be interpreted as a sum over intrinsic n-body interactions, namely, v_n^{int}. Thus, except for the trivial constant of unity (the first term), $E_V(R)$ can be regarded to be a many-body potential of the general form (1), which heretofore was not observed.

C. Rigorous bounds on the nearest-neighbor functions

Upper and lower bounds on the so-called *canonical* n-point correlation function $H_n(\mathbf{x}^m; \mathbf{x}^{p-m}; \mathbf{r}^q)$ (with $n = p+q$ and $m \le p$) for point processes in $\mathbb{R}^d$ have been found [2,51]. Since the void exclusion probability and nearest-neighbor probability density function are just special cases of H_n, then we also have strict bounds on them for such models. Let X represent either E_V or H_V and $X^{(k)}$ represent the kth term of the series for these functions. Furthermore, let

$$W^{\ell} = \sum_{k=0}^{\ell} (-1)^k X^{(k)} \tag{63}$$

be the partial sum. Then it follows that for any of the exclusion probabilities or nearest-neighbor probability density functions, we have the bounds

$$X \le W^{\ell}, \quad \text{for } \ell \text{ even}, \qquad X \ge W^{\ell}, \quad \text{for } \ell \text{ odd}. \tag{64}$$

Application of the aforementioned inequalities yields the first three successive bounds on the non-negative exclusion probability:

$$E_V(R) \le 1, \tag{65}$$

$$E_V(R) \ge 1 - \rho v_1(R), \tag{66}$$

$$E_V(R) \le 1 - \rho v_1(R) + \frac{\rho^2}{2} s_1(1) \int_0^{2R} x^{d-1} v_2^{\text{int}}(x;R) g_2(x) dx, \tag{67}$$

where $v_2^{\text{int}}(x;R) = v_1(R)\alpha(x;R)$ is the intersection volume of two d-dimensional spheres of radius R whose centers are separated by the distance x and $\alpha(x;R)$ is the scaled intersection volume given by Eq. (22). The corresponding first two nontrivial bounds on the non-negative pore-size density function $H_V(R)$ are as follows:

$$H_V(R) \le \rho s_1(R), \tag{68}$$

$$H_V(R) \ge \rho s_1(R) - \frac{\rho^2}{2} s_1(1) \int_0^{2R} x^{d-1} s_2^{\text{int}}(x;R) g_2(x) dx, \tag{69}$$

where $s_2^{\text{int}}(x;R) \equiv \partial v_2^{\text{int}}(x;R)/\partial R$ is the surface area of the intersection volume $v_2^{\text{int}}(x;R)$. Bounds on the conditional function $G_V(r)$ follow by combining the bounds above on $E_V(r)$ and $H_V(r)$ and definition (52). For example, the following bounds have been found [49]:

$$G_V(R) \le \frac{1}{1 - \rho v_1(R)}, \tag{70}$$

$$G_V(R) \geq \frac{1 - \frac{\rho}{s_1(R)} s_1(1) \int_0^{2R} x^{d-1} s_2^{\text{int}}(x;R) g_2(x) dx}{1 - \rho v_1(R) + \frac{\rho^2}{2} s_1(1) \int_0^{2R} x^{d-1} v_2^{\text{int}}(x;R) g_2(x) dx}, \tag{71}$$

which should only be applied for R such that $G_V(R)$ remains positive.

D. Truncation of the series expansions for nearest-neighbor functions for packings

For congruent sphere packings of diameter D at packing density ϕ, the infinite series expansion for $E_V(R)$ [cf. Eq. (57)] will truncate after a finite number of terms for a bounded value of the radius R. A spherical region of radius R centered at an arbitrary point in the space exterior to the spheres can contain at most n_{max} sphere centers. Therefore, series (58) truncates after $n_{max}+1$ terms, i.e.,

$$E_V(R) = 1 + \sum_{k=1}^{n_{max}} (-1)^k \frac{\rho^k}{k!} \int_{\mathbb{R}^d} g_k(\mathbf{r}_1, \ldots, \mathbf{r}_k) \times \prod_{j=1}^{k} \Theta(R - |\mathbf{x} - \mathbf{r}_j|) d\mathbf{r}_j. \tag{72}$$

For a spherical region of radius $R=D/\sqrt{3}$, $n_{max}=2$ and hence we have the exact expression that applies for $0 \leq R \leq D/\sqrt{3}$,

$$\begin{aligned} E_V(R) &= 1 - \rho v_1(R) + \frac{\rho^2}{2} s_1(1) \int_D^{2R} x^{d-1} v_2^{\text{int}}(x;R) g_2(x) dx \\ &= 1 - 2^d \phi \left(\frac{R}{D}\right)^d \\ &\quad + \frac{2^{d-1} d \phi^2}{D^d} \left(\frac{R}{D}\right)^d \int_D^{2R} x^{d-1} \alpha(x;R) g_2(x) dx. \end{aligned} \tag{73}$$

For any sphere packing for which Eq. (10) applies such that $r_2/r_1 > 2/\sqrt{3}$, we have upon use of Eq. (73) the exact result

$$E_V(R) = \begin{cases} 1 - 2^d \phi \left(\frac{R}{D}\right)^d, & 0 \leq R \leq D/2 \\ 1 - 2^d \phi \left[1 - \frac{Z}{2} \alpha(D;R)\right] \left(\frac{R}{D}\right)^d, & D/2 \leq R \geq D/\sqrt{3}, \end{cases} \tag{74}$$

where we have used the fact that $r_1=D$. Importantly, this relation applies to the densest known lattice packings of spheres, at least for dimensions in the range $1 \leq d \leq 24$.

V. REFORMULATION OF THE COVERING AND QUANTIZER PROBLEMS

A. Reformulations

Now we can reformulate the covering and quantizers problems in terms of the void exclusion probability. In particular, the covering problem asks for the point process in $\mathbb{R}^d$ at unit density ($\rho=1$) that minimizes the support of the radial function $E_V(R)$. We define $\mathcal{R}_c^{min}$ as the smallest possible value of the covering radius $\mathcal{R}_c$ among all point processes for which $E_V(R)=0$, which we call the *minimal covering radius*. This is indeed a special ground state in which the "energy" is identically zero [i.e., $E_V(\mathcal{R}_c^{min})=0$] [52]. Depending on the space dimension d, this special ground state will involve one-body interactions, the first two terms of Eq. (62), one- and two-body interactions, the first three terms of Eq. (62), one-, two-, and three-body interactions, the first four terms of Eq. (62), etc., and will truncate at some particular level, provided that $E_V(R)$ for the point process has compact support. The minimal covering radius $\mathcal{R}_c^{min}$ increases with the space dimension d and, generally speaking, the highest-order n-body interaction required to fully characterize the associated $E_V(R)$ increases with d. Note that for a particular point process, twice the covering radius $2\mathcal{R}_c$ can be viewed as the "effective interaction range" between any pair of points, since the intersection volume $v_2^{\text{int}}(r_{ij};R)$, which appears in expression (62) for $E_V(R)$, is exactly zero for any pair separation $r_{ij} > 2\mathcal{R}_c$; moreover, for such pair separations v_n^{int} can be written purely in terms of the lower-order intersection volume v_{n-1}^{int}. Therefore, because $v_2^{\text{int}} \geq v_n^{\text{int}}$ for $n \geq 3$, the effective interaction range between any n points for $n \geq 3$ is still given by $2\mathcal{R}_c$.

The quantizer problem asks for the point process in $\mathbb{R}^d$ at unit density that minimizes the scaled average squared error $\mathcal{G}$ defined as

$$\mathcal{G} = \frac{1}{d}\langle R^2 \rangle = \frac{1}{d} \int_0^\infty R^2 H_V(R) dR = \frac{2}{d} \int_0^\infty R E_V(R) dR. \tag{75}$$

We will call the minimal error $\mathcal{G}_{min}$. Thus, we seek the ground state of the many-body interactions that are involved upon substitution of Eq. (62) into Eq. (75). Again, depending on the dimension, this many-body energy will truncate at some particular level, provided that $E_V(R)$ has compact support. As d increases, successively higher-order interactions in expression (62) must be incorporated to completely characterize $E_V(R)$.

B. Explicit calculations for some common lattices using these reformulations

It is instructive to express explicitly the void exclusion probabilities for some common lattices and use these functions to evaluate explicitly their corresponding covering densities and scaled average squared errors in the first three space dimensions.

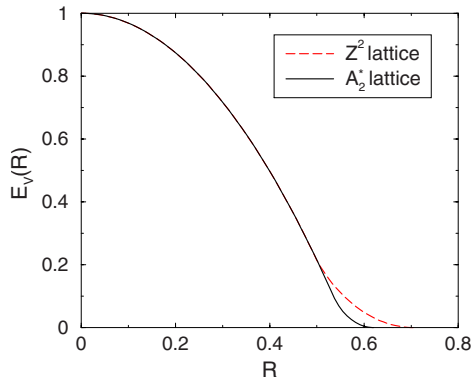

FIG. 6. (Color online) The void exclusion probabilities $E_V(R)$ for the $\mathbb{Z}^2$ (square) and $A_2 \equiv A_2^*$ (triangular) lattices have support up to the covering radii $\mathcal{R}_c = \sqrt{2}/2 = 0.7071\ldots$ and $\mathcal{R}_c = \sqrt{2}/3^{3/4} = 0.6204\ldots$, respectively, at unit number density ($\rho = 1$).

In the simplest case of one dimension, the series expansion for $E_V(R)$ [cf. Eq. (62)] for the integer lattice $\mathbb{Z}$ truncates after only one-body terms. At unit number density ($\rho = 1$), it is trivial to show that

$$E_V(R) = \begin{cases} 1 - v_1(R), & 0 \le R \le \mathcal{R}_c \\ 0, & R \ge \mathcal{R}_c, \end{cases} \tag{76}$$

where the covering radius $\mathcal{R}_c = 1/2$, $v_1(R) = 2R$, and the nearest-neighbor distance from a lattice point is unity. Using definitions (36) and (75) in combination with Eq. (76) yields the covering density and scaled average squared error, respectively, for the optimal integer lattice:

$$\theta = 1, \tag{77}$$

$$\mathcal{G} = \frac{1}{12} = 0.083\ 333\ldots. \tag{78}$$

Let us now determine the void exclusion probabilities for the $\mathbb{Z}^2$ (square) and $A_2 \equiv A_2^*$ (triangular) and lattices for R up to their respective covering radii for which $E_V(R) = 0$. For these lattices, the series expression (62) for $E_V(r)$ truncates after two-body terms. For the square and triangular lattices at $\rho = 1$,

$$E_V(R) = \begin{cases} 1 - v_1(R), & 0 \le R \le r_1/2 \\ 1 - v_1(R) + 2v_2^{\text{int}}(r_1;R), & r_1/2 \le R \le \mathcal{R}_c \\ 0, & R \ge \mathcal{R}_c, \end{cases} \tag{79}$$

where r_1 is the nearest-neighbor distance from a lattice point and the covering radius $\mathcal{R}_c$, equal to one half of the next-nearest-neighbor distance, which we will denote by r_2. For the square and triangular lattices at $\rho = 1$, $r_1 = 1$ and $\mathcal{R}_c = \sqrt{2}/2 = 0.7071\ldots$, and $r_1 = \sqrt{2}/3^{1/4} = 1.0745\ldots$ and $\mathcal{R}_c = \sqrt{2}/3^{3/4} = 0.6204\ldots$, respectively. Figure 6 provides plots of $E_V(R)$ for these two $d = 2$ lattices. Employing definitions (36) and (75) in combination with Eq. (79) provides the covering density and scaled average squared error, respectively, for the $\mathbb{Z}^2$ lattice:

$$\theta = \frac{\pi}{2} = 1.570\ 79\ldots, \tag{80}$$

$$\mathcal{G} = \frac{1}{12} = 0.083\ 333\ldots. \tag{81}$$

Similarly, the corresponding equations for the A_2 lattice yields the covering density and scaled average squared error, respectively, for this optimal structure:

$$\theta = \frac{2\pi}{3^{1/3}} = 1.209\ 19\ldots, \tag{82}$$

$$\mathcal{G} = \frac{5}{36\sqrt{3}} = 0.080\ 18\ldots. \tag{83}$$

It is also useful to express explicitly the void exclusion probabilities for the $\mathbb{Z}^3$ (simple-cubic) and A_3^* (bcc) lattices for R up to their respective covering radii for which $E_V(R) = 0$. It turns out that calculating $E_V(R)$ in the case of the simple-cubic lattice is more complicated than that for the bcc lattice because the former involves up through four-body terms, i.e., v_4^{int}. However, the symmetry of the geometry for $\mathbb{Z}^3$ enables one to express v_4^{int} purely in terms of v_2^{int} and v_3^{int}. The calculation of $E_V(R)$ does not involve four-body terms. For the simple-cubic lattice at $\rho = 1$,

$$E_V(R) = \begin{cases} 1 - v_1(R), & 0 \le R \le r_1/2 \\ 1 - v_1(R) + 3v_2^{\text{int}}(r_1;R), & r_1/2 \le R \le r_2/2 \\ 1 - v_1(R) + 3v_2^{\text{int}}(r_1;R) + 3v_2^{\text{int}}(r_2;R) - 6v_3^{\text{int}}(r_1,r_1,r_2;R), & r_2/2 \le R \le \mathcal{R}_c \\ 0, & R \ge \mathcal{R}_c, \end{cases} \tag{84}$$

where $r_1 = 1$, $r_2 = \sqrt{2} = 1.4142\ldots$, $\mathcal{R}_c = \sqrt{3}/2 = 0.8660\ldots$, and $v_3^{\text{int}}(r,s,t;R)$ is explicitly given by Eq. (B1) in Appendix B for triangles of side lengths r, s, and t. Here, we have used the fact that for $r_2/2 \le R \le \mathcal{R}_c$, $v_4^{\text{int}}(r_1,r_1,r_2,r_2) = 6v_3^{\text{int}}(r_1,r_1,r_2) - 3v_2^{\text{int}}(r_2)$. Using definitions (36) and (75) in combination with Eqs. (84) yields the covering density and scaled average squared error, respectively, for the $\mathbb{Z}^3$ lattice:

$$\theta = \frac{\pi\sqrt{3}}{2} = 2.720\ 69\ldots, \tag{85}$$

$$\mathcal{G} = \frac{1}{12} = 0.083\ 333\ldots. \tag{86}$$

For the bcc lattice at $\rho=1$,

$$E_V(R) = \begin{cases} 1 - v_1(R), & 0 \le R \le r_1/2 \\ 1 - v_1(R) + 4v_2^{\text{int}}(r_1;R), & r_1/2 \le R \le r_2/2 \\ 1 - v_1(R) + 4v_2^{\text{int}}(r_1;R) + 3v_2^{\text{int}}(r_2;R), & r_2/2 \le R \le R_T \\ 1 - v_1(R) + 4v_2^{\text{int}}(r_1;R) + 3v_2^{\text{int}}(r_2;R) - 12v_3^{\text{int}}(r_1,r_1,r_2;R), & R_T \le R \le \mathcal{R}_c \\ 0, & R \ge \mathcal{R}_c, \end{cases} \tag{87}$$

where $r_1=\sqrt{3}/4^{1/3}=1.0911\ldots$, $r_2=4^{1/6}=1.2599\ldots$, $\mathcal{R}_c=\sqrt{5}/2^{5/3}=0.7043\ldots$, and $R_T=3/2^{13/6}=0.6681\ldots$ is the circumradius of a triangle of side lengths r_1, r_1, and r_2, the general expression of which is given by Eq. (B2) in Appendix B. Employing definitions (36) and (75) in combination with Eqs. (87) provides the covering density and scaled mean-squared error, respectively, for the $\mathbb{A}_3^*$ lattice:

$$\theta = \frac{\pi \times 5^{3/2}}{24} = 1.463\ 50\ldots, \tag{88}$$

$$\mathcal{G} = \frac{19}{192 \times 2^{1/3}} = 0.078\ 543\ldots. \tag{89}$$

Figure 7 provides plots of $E_V(R)$ for the simple-cubic and bcc three-dimensional lattices.

C. Remarks about higher dimensions

We see that the best known solutions to the covering and quantizer problems are identical for the first three space dimensions. However, there is no reason to expect for the optimal solutions for these two problems to be the same in higher dimensions, except for $d=24$ for reasons mentioned in Sec. III E. Although both problems involve ground states associated with the "many-body interaction" function $E_V(R)$, such that it possesses compact support for finite d, the precise shape of the function $E_V(R)$ for a particular point configuration is crucial in determining its first moment or quantizer error. By contrast, the best covering seeks to find the point configuration that minimizes the support of $E_V(R)$ without regard to its shape.

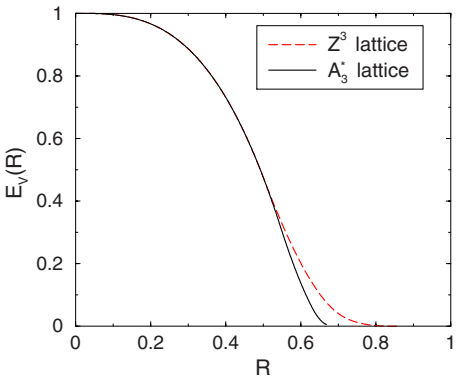

FIG. 7. (Color online) The void exclusion probabilities $E_V(R)$ for the $\mathbb{Z}^3$ (simple-cubic) lattice and A_3^* (bcc) lattice have support up to the covering radii $\mathcal{R}_c=\sqrt{3}/2=0.8660\ldots$ and $\mathcal{R}_c=\sqrt{5}/2^{5/3}=0.7043\ldots$, respectively, at unit number density ($\rho=1$).

VI. RESULTS FOR THE COVERING PROBLEM

Saturated sphere packings in $\mathbb{R}^d$ should provide relatively thin coverings. Surrounding every sphere of diameter D in any saturated packing of congruent spheres in $\mathbb{R}^d$ at packing density ϕ_s by spheres of radius D provides a covering of $\mathbb{R}^d$, and thus the associated covering density θ_s is given by

$$\theta_s = \rho_s v_1(D) = 2^d \phi_s, \tag{90}$$

where ρ_s and $\phi_s=\rho_s v_1(D/2)$ are the number density and packing density, respectively, of the saturated packing. What is the thinnest possible covering associated with a saturated packing? It immediately follows that the thinnest coverings among saturated congruent sphere packings in $\mathbb{R}^d$ are given by the saturated packings that have the minimal packing density ϕ_s^* in that space dimension and have covering density

$$\theta_s^* = 2^d \phi_s^*. \tag{91}$$

We can also bound the packing density ϕ_s of any saturated sphere packing in $\mathbb{R}^d$ from above using upper bounds on the covering density.

Lemma 1. The density ϕ_s of any saturated sphere packing in $\mathbb{R}^d$ is bounded from above according to

$$\phi_s \le \frac{5d}{2^d} + \frac{d\ln(d)}{2^d} + \frac{d\ln[\ln(d)]}{2^d}. \tag{92}$$

The proof is trivial in light of the upper bound (42) on the covering density and relation (90).

The standard RSA sphere packing is a time-dependent process produced by randomly, irreversibly, and sequentially placing nonoverlapping spheres into a large region $\mathcal{V}\subset\mathbb{R}^d$ [53]. Initially, this large region is empty of sphere centers, and subsequently spheres are added provided each attempted placement of a sphere does not overlap an existing sphere in the packing. If an attempted placement results in an overlap, further attempts are made until the sphere can be added to the packing at that time without violating the impenetrability constraint. For identical d-dimensional RSA spheres, the filling process terminates at the *saturation limit* at infinitely long times in the infinite-volume limit. Thus, in this limit, the RSA packing is a saturated packing. The saturation density ϕ_s can only be determined exactly in one dimension, where it is known to be $\phi_s=0.747\,597\ldots$ [54]. In higher dimensions, the saturation density can only be determined from computer simulations. Earlier work focused on two and three dimensions, where it was found that $\phi_s\approx 0.547$ [55] and $\phi_s\approx 0.38$ [56], respectively. More recent numerical work has reported RSA saturation densities for the first six space dimensions [38]. It is important to emphasize that upper bound (92) provides a very poor estimate of the RSA saturation density; for example, for $d=3$, it gives an upper bound greater than unity (2.322 24, which is about 6.1 times larger than the value obtained from simulations) and for $d=6$, it provides the upper bound 0.691 402, which is about 7.3 times larger than the value obtained from simulations [38]. Thus, bound (92) could only be realized by RSA saturated packings, if at all, in high dimensions.

Therefore, it is useful here to compute the corresponding covering densities for RSA packings. The numerical data for RSA saturation densities for $2\leq d\leq 6$ reported in Ref. [38] were well approximated (with a correlation coefficient of 0.999) by the following form:

$$\phi_s=\frac{c_1}{2^d}+\frac{c_2 d}{2^d}, \tag{93}$$

where $c_1=0.202\,048$ and $c_2=0.973\,872$. This can be used to estimate the RSA saturation densities for $d\geq 7$. However, even though the upper bound (92) on the packing density of a saturated sphere packing grossly overestimates the RSA value for the first six space dimensions, we include in the fit function for ϕ_s a $d\ln(d)$ correction, which will lead to a more conservative estimate of the covering density, as explained shortly [57]. Including such a term, we find the following fitted function for the saturated RSA packing density:

$$\phi_s=\frac{a_1}{2^d}+\frac{a_2 d}{2^d}+\frac{a_3 d\ln(d)}{2^d}, \tag{94}$$

with a correlation coefficient of 0.999, where $a_1=0.350\,648$, $a_2=0.876\,60$, and $a_3=0.041\,428$, does as well as Eq. (93) for $2\leq d\leq 6$. Since Eq. (94) predicts slightly higher densities than Eq. (93) for $7\leq d\leq 24$ [58], we use it to obtain the corresponding estimate of the RSA covering density, namely,

$$\theta_s=a_1+a_2 d+a_3 d\ln(d), \tag{95}$$

which is a slightly more conservative estimate since Eq. (93) would yield a slightly thinner covering density.

TABLE VI. Covering density θ_s for RSA packings at the saturation state in selected dimensions. The values for the first six space dimensions are obtained from the reported saturated density values given in Refs. [38,54] and using Eq. (90). The values reported for $d\geq 7$ are estimates obtained from the fitting formula (95). Included in the table are the corresponding saturation packing densities.

Dimension d	Covering density θ_s	Packing density ϕ_s
1	1.4952	0.74759
2	2.1880	0.54700
3	3.0622	0.38278
4	4.0726	0.25454
5	5.1526	0.16102
6	6.0121	0.09394
7	7.0512	0.05508
8	8.0526	0.03145
9	10.0706	0.01769
10	11.0860	0.009834
12	12.1052	0.002955
16	16.2141	2.4740×10^{-4}
17	17.2482	1.3159×10^{-4}
18	18.2848	6.9751×10^{-5}
24	24.5489	1.4632×10^{-6}

In Table VI, we provide estimates of the RSA covering densities for selected dimensions up through $d=24$. The covering density for $d=1$ is determined from Reńyi's exact saturation packing density value [54] and multiplying it by 2. The values for $2\leq d\leq 6$ are obtained from the reported saturated density values in Ref. [38] and multiplying each density value by 2^d. The values reported for $d\geq 7$ are estimates obtained from the fitting formula (95). Comparing Table VI to Table III for the best known coverings, we see that saturated RSA packings not only provide relatively thin coverings but also putatively represent the first nonlattices that yield thinner coverings than the best known lattice coverings beginning in about dimension 17. This suggests that saturated RSA packings may be thinner than the previously best known coverings for $17\leq d\leq 23$ and probably for some dimensions greater than 24.

VII. RESULTS FOR THE QUANTIZER PROBLEM

Using the successive lower and upper bounds on the void exclusion probability function $E_V(R)$ given in the previous section, we can, in principle, derive corresponding bounds on the minimal error $\mathcal{G}_{min}$. Moreover, one can obtain a variety of upper bounds on $\mathcal{G}_{min}$ using our approach by utilizing the exact form of the void exclusion probability, when it is known, for some point process at unit density. Since a general point process must have an error $\mathcal{G}$ that is generally larger than the minimal $\mathcal{G}_{min}$, it trivially follows that

$$\mathcal{G}_{min}\leq\mathcal{G}. \tag{96}$$

A. Revisiting Zador's bounds

To illustrate how we can obtain bounds on $\mathcal{G}_{min}$ using our approach, we begin by rederiving the following bounds due to Zador [46]:

$$\frac{1}{(d+2)\pi}\Gamma(1+d/2)^{2/d} \le \mathcal{G}_{min} \le \frac{1}{d\pi}\Gamma(1+d/2)^{2/d}\Gamma(1+2/d). \tag{97}$$

Consider the lower bound first. Combination of relation (75) and lower bound (66) yields at unit density

$$\mathcal{G}_{min} \ge \frac{2}{d}\int_0^{R_0} R[1-v_1(R)]dR = \frac{1}{(d+2)\pi}\Gamma(1+d/2)^{2/d}, \tag{98}$$

which is seen to be equal to Zador's lower bound. Here, $R_0=\Gamma(1+d/2)^{1/d}/\sqrt{\pi}$ is the zero of $1-v_1(R)$. It is clear that a sphere of radius R_0 has the smallest second moment of inertia of any solid d-dimensional solid, and hence establishes the lower bound. The simplest example of a point process for which $E_V(R)$ is known is the Poisson point process [cf. Eq. (60)]. Substitution of Eq. (60) into Eq. (96) at unit density yields

$$\mathcal{G}_{min} \le \frac{2}{d}\int_0^{\infty} R\exp(-v_1(R))dR = \frac{1}{d\pi}\Gamma(1+d/2)^{2/d}\Gamma(1+2/d), \tag{99}$$

which is seen to be equal to Zador's upper bound. These derivations of the inequalities stated in Eq. (97) appear to be much simpler than the ones presented by Zador.

In the large-d limit, Zador's upper and lower bounds become identical, and hence one obtains the exact asymptotic result

$$\mathcal{G}_{min} \to \frac{1}{2\pi e} = 0.058\,550\ldots \quad \text{as} \quad d\to\infty. \tag{100}$$

The convergence of Zador's bounds to the exact asymptotic limit is to be contrasted with the sphere-packing problem in which the best upper and lower bounds on the maximal density become exponentially far apart in the high-dimensional limit.

B. Improved upper bounds

Improved upper bounds on $\mathcal{G}_{min}$ can be obtained by considering those point processes corresponding to a sphere packing for which the minimal pair separation is D and lower bounds on the conditional function $G_V(R)$ for $R \ge D/2$. In what follows, we present two different upper bounds on $\mathcal{G}_{min}$ based on this idea that improve upon Zador's upper bound.

For any packing of identical spheres with diameter D, the following exact relations on the nearest-neighbor quantities apply for $R \le D/2$ [2]:

$$E_V(R) = 1-2^d\phi\left(\frac{R}{D}\right)^d, \quad H_V(R) = \frac{d2^d\phi}{D}\left(\frac{R}{D}\right)^{d-1}, \quad G_V(R) = \frac{1}{1-2^d\phi\left(\frac{R}{D}\right)^d}, \quad 0 \le R \le D/2. \tag{101}$$

Observe that $G_V(R)$ is a monotonically increasing function of R in the interval $[0,D/2]$. From these equalities, it immediately follows that

$$E_V(D/2) = 1-\phi, \quad H_V(D/2) = \frac{2d\phi}{D}, \quad G_V(D/2) = \frac{1}{1-\phi}. \tag{102}$$

Consider now the class of sphere packings for which the conditional nearest-neighbor function is bounded from below according to

$$G_V(R) \ge \frac{1}{1-\phi} \quad \text{for all} \quad R \ge D/2. \tag{103}$$

This class of packings includes equilibrium (Gibbs) ensembles of hard spheres along the disordered fluid branch of the phase diagram [2,30,48], nonequilibrium disordered sphere packings, such as the ghost random sequential addition (RSA) process [15], and a large class of lattice packings of spheres, as will be described below. In the equilibrium cases, it is known that $G_V(R)$ is a monotonically increasing function of R for $d \ge 2$, and thus using this property together with the equality $G_V(D/2)=1/(1-\phi)$ [cf. Eq. (102)] it means that the lower bound (103) is obeyed. For one-dimensional equilibrium "rods," bound (103) is sharp (exact) $G_V(R)$ for all realizable $\phi \in [0,1]$. A bound of type (103) was used to bound the related particle mean nearest-neighbor distance from above for different classes of sphere packings for all d [48].

Using definition (54) and inequality (103), the void exclusion probability function obeys the following upper bound for $R \ge D/2$:

$$E_V(R) \le (1-\phi)\exp\left\{-\frac{2^d\phi}{1-\phi}\left[\left(\frac{R}{D}\right)^d - \frac{1}{2^d}\right]\right\}, \quad R \ge D/2. \tag{104}$$

Since any upper bound on the non-negative function $E_V(R)$ leads to an upper bound on its first moment, we then have upon use of Eqs. (96), (101), and (104) the upper bound

$$\mathcal{G}_{min} \le \frac{4[\phi\Gamma(1+d/2)]^{2/d}}{d\pi}\left[\frac{(d+2(1-\phi))}{4(2+d)} + \frac{(1-\phi)}{2d}\left(\frac{1-\phi}{\phi}\right)^{2/d}\exp\left(\frac{\phi}{1-\phi}\right)\Gamma\left(\frac{2}{d},\frac{\phi}{1-\phi}\right)\right], \tag{105}$$

where $\Gamma(s,x) \equiv \int_x^{\infty} t^{s-1}e^{-t}dt$ is the incomplete gamma function. Observe that the prefactor multiplying the bracketed expression is D^2/d, where in light of Eqs. (14) and (16) $D=2[\phi\Gamma(1+d/2)]^{1/d}/\sqrt{\pi}$, assuming unit number density. Note also that the upper bound (105) depends on a single param-

eter, namely, the packing density ϕ. Thus, there is an optimal packing density $\phi_{opt} \in [0, \phi_{max}]$ that yields the best (smallest) upper bound for any particular d, where ϕ_{max} is the maximal packing density. Since the right side of the inequality is a monotonically decreasing function of ϕ for any d, then the optimal density ϕ_{opt} is, in principle, given by ϕ_{max}. It is noteworthy that the upper bound (105) for the optimal choice $\phi=\phi_{max}$ may still be valid for a packing even if bound (104), upon which it is based, is violated for R on the order of D because the exponential tail can more than compensate for such a violation such that the error [first moment of $E_V(R)$] is overestimated. Observe also that, because

$$\Gamma\left(\frac{2}{d}, \frac{\phi}{1-\phi}\right) = \frac{1}{4}\left[\left(\frac{1-\phi}{\phi}\right)^{2/d}\right] + \mathcal{O}(1) \quad (d \to \infty), \tag{106}$$

the upper bound (105) tends to the exact asymptotic result (100) of $(2\phi e)^{-1}$.

Before discussing the optimal bounds, it is useful to begin with an application of the upper bound (105) for the *suboptimal* case of a disordered sphere packing, namely, the aforementioned ghost RSA packing process [15], which we now show generally improves on Zador's upper bound. This represents the only exactly solvable disordered sphere-packing model for all realizable densities and in any dimension, as we now briefly describe. The ghost RSA packing process involves a (time-dependent) sequential addition of spheres in space subject to the nonoverlap condition. Not only is an attempted addition of a sphere rejected if it overlaps an existing sphere of the packing, it is also rejected if it overlaps any previously rejected sphere (called a ghost sphere). Unlike the standard RSA packing, the ghost RSA packing does not become a saturated packing in the infinite-time limit. All of the n-particle correlation functions for this nonequilibrium model have been obtained analytically for any d, time t, and for all realizable densities. For example, one can show that the maximal density (achieved at infinite time) is given by

$$\phi = \frac{1}{2^d}, \tag{107}$$

and the associated pair-correlation function is

$$\rho^2 g_2(r) = \frac{2\Theta(r-D)}{2-\alpha(r;D)}, \tag{108}$$

where $\Theta(x)$ is the unit step function, equal to zero for $x<0$ and unity for $x \geq 1$. It is straightforward to verify that the upper bound on the exclusion probability $E_V(R)$ for this infinite-time case obtained by using Eq. (108) in inequality (67) is always below the upper bound (104). Therefore, the upper bound (105) is valid at the maximal density, i.e., at $\phi=1/2^d$, we have

$$\mathcal{G}_{min} \leq \frac{[\Gamma(1+d/2)]^{2/d}}{d\pi}\left[\frac{[d+2(1-1/2^d)]}{4(2+d)} + \frac{2(1-1/2^d)^{(2+d)/d}}{d}\exp\left(\frac{1}{2^d-1}\right)\Gamma\left(\frac{2}{d}, \frac{1}{2^d-1}\right)\right]. \tag{109}$$

For $d=1$, 2, and 3, this upper bound yields 0.166 666…, 0.124 339…, and 0.106 797…, respectively, which is to be compared to Zador's upper bound, which gives 0.5, 0.159 154…, and 0.115 802…, respectively. We note that in the large-d limit, the upper bound (109) yields the exact asymptotic result (100), which implies that the upper bound (104) on $E_V(R)$ becomes exact for ghost RSA packings, tending to the unit step function in this asymptotic limit, i.e.,

$$E_V(R) \to \Theta(r-D) \quad (d \to \infty). \tag{110}$$

This asymptotic result implies the following corresponding one for the void nearest-neighbor probability density function:

$$H_V(R) \to \delta(r-D) \quad (d \to \infty). \tag{111}$$

We now return to finding the optimal (smallest) upper bound (105) for each dimension. For $d=1$, the optimal density is $\phi_{opt}=\phi_{max}=1$, which produces the sharp bound

$$\mathcal{G}_{min} \leq \frac{1}{12} = 0.083\ 333\ldots. \tag{112}$$

This bound is exact in this case because inequality (103) is exact for all realizable densities for equilibrium hard rods, including at $\phi=1$, which corresponds to the optimal integer lattice packing. This is to be contrasted with Zador's upper bound, which yields 1/2 for $d=1$ and is far from the exact result. The improved upper bound (105) in the higher dimensions reported in Table VII is obtained by evaluating it at the densities of the densest known lattice packings in these respective dimensions [18]. We note that it is only for optimal triangular lattice packing in $\mathbb{R}^2$ that the upper bound (104) on $E_V(R)$ is violated pointwise for a small range of R around $R/D=1/2$ [inequality (104) is obeyed for $R/D \geq 0.539$ and in the vicinity of $R/D=0.5$], but the exponential tail associated with Eq. (104) more than compensates for this narrow pointwise violation, resulting in a strict upper bound on the first moment of $E_V(R)$ i.e., (105) remains a strict upper bound for $d=2$. Using relation (74) and lattice coordination properties, it is easily verified that Eq. (104) is a strict upper bound on the void exclusion probability for the densest known lattice packings for all $R \geq D/2$ and $3 \leq d \leq 24$ as well as $d=1$, and hence inequality (105) provides a strict upper bound on the scaled error for all of these lattices. For illustration purposes, we compare in Fig. 8 the exact result for E_V obtained from Eq. (74) to estimate (104) for the cases $d=2$ and $d=4$ for $1/2 \leq R/D \leq 1/\sqrt{3}$. The upper bound (105) is generally appreciably tighter than Zador's upper bound for low to moderately high dimensions.

TABLE VII. Comparison of the best known quantizers in selected dimensions to the conjectured lower bound due to Conway and Sloane and the improved upper bound (105).

d	Quantizer	Scaled error $\mathcal{G}$	Conjectured lower bound	Improved upper bound
1	$A_1^*=\mathbb{Z}$	0.083333	0.083333	0.083333
2	$A_2^*\equiv A_2$	0.080188	0.080188	0.080267
3	$A_3^*\equiv D_3^*$	0.078543	0.077875	0.079724
4	$D_4^*\equiv D_4$	0.076603	0.07609	0.078823
5	Λ_5^{2*}	0.075625	0.07465	0.078731
6	E_6^*	0.074244	0.07347	0.077779
7	Λ_7^{3*}	0.073116	0.07248	0.076858
8	$E_8^*=E_8$	0.071682	0.07163	0.075654
9	L_9^{AE}	0.071626	0.070902	0.075552
10	D_{10}^+	0.070814	0.070405	0.074856
12	$K_{12}^*\equiv K_{12}$	0.070100	0.06918	0.073185
16	$\Lambda_{16}^*\equiv\Lambda_{16}$	0.068299	0.06759	0.070399
24	$\Lambda_{24}^*=\Lambda_{24}$	0.065771	0.06561	0.067209

C. Results for saturated packings

For any saturated packing of identical spheres of diameter D, $E_V(R)$ by definition is exactly zero for R beyond the diameter, i.e.,

$$E_V(R)=0, \quad R\geq D. \tag{113}$$

In the particular case of saturated RSA packings, the void exclusion probability can computed using the same techniques described in Ref. [38] for the first six space dimensions. These results are summarized in Fig. 9. The corresponding quantizer errors for these dimensions are listed in Table VIII. We see that the discrepancies between the saturated RSA quantizer error improves as d increases as compared to the best known quantizer error reported in Table IV.

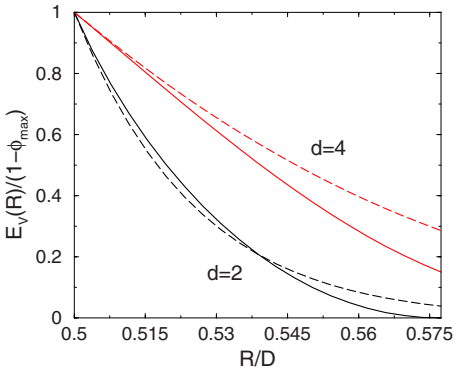

FIG. 8. (Color online) Comparison of the exact result for E_V scaled by $1-\phi_{max}$ for the optimal lattice packings for $d=2$ (A_2^*) and $d=4$ (D_4), as obtained from Eq. (74), for $1/2\leq R/D\leq 1/\sqrt{3}$ (solid curves) to the corresponding estimates obtained from Eq. (104) for these cases (dashed curves). It is only for the case $d=2$ that estimate (104) is not a rigorous pointwise upper bound on the exact void exclusion probability for $1\leq d\leq 24$, and, likely, for all $d>24$. The exponential tail associated with (104) more than compensates for the narrow pointwise violation for the special case $d=2$, resulting in a strict upper bound on the first moment of $E_V(R)$, i.e., (105) remains a strict upper bound for $d=2$.

Lemma 2. Saturated sphere packings in $\mathbb{R}^d$ possess void nearest-neighbor functions that tend to the following high-dimensional asymptotic behaviors:

$$E_V(R)\to\Theta(r-D), \quad H_V(R)\to\delta(r-D) \quad (d\to\infty). \tag{114}$$

For any saturated packing at packing density ϕ_s, it is clear that $E_V(R)$ is bounded from above for $R\geq D/2$ as follows:

$$E_V(R)\leq 1-\phi_s, \quad D/2\leq R\leq D. \tag{115}$$

Let $\mathcal{G}_s$ denote the scaled dimensionless quantizer error for a saturated packing. Combination of the expression for $E_V(R)$ in Eqs. (101) and (115) yields the following upper bound on $\mathcal{G}_s$:

$$\mathcal{G}_s\leq\frac{4[\phi_s\Gamma(1+d/2)]^{2/d}}{d\pi}\left[\frac{[d+2(1-\phi_s)]}{4(2+d)}+\frac{3(1-\phi_s)}{8}\right]. \tag{116}$$

The fact that this upper bound becomes exact in the high-dimensional limit [that is, it tends to $(2\pi e)^{-1}$] implies that

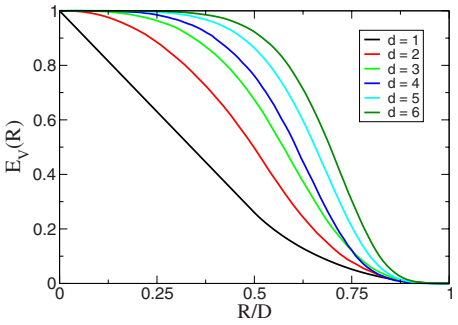

FIG. 9. (Color online) The void exclusion probability $E_V(R)$ for saturated RSA packings of congruent spheres of diameter D for the first six space dimensions.

TABLE VIII. The quantizer errors for saturated RSA packings in the first six space dimensions. We denote by $\mathcal{G}_s$ the quantizer error for such saturated packing.

Dimension d	Quantizer error $\mathcal{G}_s$
1	0.11558
2	0.09900
3	0.09232
4	0.08410
5	0.07960
6	0.07799

$E_V(R)$ and $H_V(R)$ for a saturated packing tend to the unit step function and radial delta function, as specified by Eq. (114). Not surprisingly, bound (116) is not that tight in relatively low dimensions.

VIII. CONCLUDING REMARKS AND DISCUSSION

We have reformulated the covering and quantizer problems as the determination of the ground states of interacting point particles in $\mathbb{R}^d$ that generally involve single-body, two-body, three-body, and higher-body interactions; see Sec. V. The n-body interaction is directly related to a purely geometrical problem, namely, the intersection volume of n spheres of radius R centered at n arbitrary points of the system in $\mathbb{R}^d$. This was done by linking the covering and quantizer problems to certain optimization problems involving the void nearest-neighbor functions. This reformulation allows one to employ theoretical and numerical optimization techniques to solve these energy minimization problems.

A key finding is that disordered saturated sphere packings provide relatively thin coverings and may yield thinner coverings than the best known lattice coverings in sufficiently large dimensions. In the case of the quantizer problem, we derived improved upper bounds on the quantizer error that utilize sphere-packing solutions. These improved bounds are generally substantially sharper than an existing upper bound due to Zador in low to moderately large dimensions. Moreover, we showed that disordered saturated sphere packings yield relatively good quantizers. Our reformulation helps to explain why the known solutions of quantizer and covering problems are identical in the first three space dimensions and why they can be different for $d \geq 4$. In the first three space dimensions, the best known solutions of the sphere-packing and number-variance problems (or their dual solutions) are directly related to those of the covering and quantizer problems, but such relationships may or may not exist for $d \geq 4$, depending on the peculiarities of the dimensions involved. It is clear that as d becomes large, the quantizer problem becomes the easiest to solve among the four ground-state problems considered in this paper since, unlike the other three problems, the asymptotic quantizer error tends to the same limit independent of the configuration of the point process.

The detection of gravitational waves from various astrophysical sources has and will be searched for in the output of interferometric networks [59] by correlating the noisy output of each interferometer with a set of theoretical waveform templates [26]. Depending on the source, the parameter space is generally multidimensional and can be as large as $d=17$ or larger for inspiraling binary black holes. The templates must *cover* the space and the challenge is to place them in some optimal fashion such that the fewest templates are used to reduce computational cost without reducing the detectability of the signals.

Optimal template placement for gravitational wave data analysis has proved to be highly nontrivial. One solution proposed for the optimal placement in flat (Euclidean) space is to simply use the optimal solution to the covering problem [26]. However, this requires every point in the parameter space to be covered by at least one template, which rapidly becomes inefficient in higher dimensions when optimal lattice covering solutions are employed. Another approach to template placement consists of relaxing the strict requirement of complete coverage for a given mismatch, and instead requires coverage only with a certain confidence [26]. Such stochastic approaches have involved randomly placing templates in the parameter space, accompanied by a "pruning" step in which "redundant" templates, which are deemed to lie too close to each other, are removed [60]. The pruning step may be a complication that can be avoided, as discussed below. Another approach is to place spherical templates down according to a Poisson point process [61], which has been claimed to provide good solutions for $d > 10$. The problem with the latter approach is that there will be numerous multiple overlaps of templates, which only increase as the number density of templates (intensity of the Poisson point process) is increased in order to cover as much of the space as is computationally feasible.

The results of the present study suggest alternative solutions to the optimal template construction problem. First, we remark that if the covering of space by the templates is relaxed, then it is possible that the optimal lattice quantizers could serve as good solutions in relatively low dimensions ($d \leq 10$) because the mean-square error is minimized. Second, in such relatively low dimensions, we have shown that saturated RSA sphere packings provide both relatively good coverings and quantizers, and hence may be useful in template-based constructions for the search of gravitational waves. Indeed, we have shown that saturated RSA sphere packings are expected to become better solutions as d becomes large. However, for $d \geq 10$, it will be computationally costly to create truly saturated packings, which by definition provide coverings of space (see Sec. VI). However, the existing stochastic approaches do not require complete coverage of space and hence an *unsaturated* RSA sphere packing that gets relatively close to the saturation state might still be more computationally efficient than either the random placement and pruning technique [60] (because pruning is unnecessary) or the Poisson placement procedure [61] (because far fewer spheres need to be added). Moreover, when the template parameter space is curved, which occurs in practice [61], the RSA sphere packing would be computational faster to adapt than lattice solutions.

In future work, we will explore whether our reformulations of the covering and quantizer problems as ground-state problems of many-body interactions of form (1) can facili-

tate the search for better solutions to these optimization tasks. Clearly, a computational challenge in high dimensions will be the determination of the intersection volume v_n^{int} of n spheres of radius R at n different locations in $\mathbb{R}^d$ for sufficiently large n. However, it is possible that the series representations (62) for $E_V(R)$ and bounds on this quantity [cf. Sec. IV C] can be used to devise useful approximations of the monotonic function $E_V(R)$, which should be zero for $R \geq 2\mathcal{R}_c$, where $\mathcal{R}_c$ is the bounded covering radius. Such an approximation could be employed to evolve an initial guess of the configuration of points within a fundamental cell to useful but suboptimal solutions, which upon further refinement could suggest novel solutions. In short, the implications of our reformulations to discover better solutions to the covering and quantizer problems in selected dimensions have yet to be fully investigated and deserve future attention.

ACKNOWLEDGMENTS

I am very grateful to Yang Jiao and Chase Zachary for their assistance in creating many of the figures for this manuscript and for many useful discussions. I thank Andreas Strömbergsson and Zeev Rudnick for their generous help in providing efficient algorithms to compute the Epstein zeta function for $d=12$, 16, and 24. I also thank Henry Cohn for introducing me to the quantizer problem as well as for many helpful discussions. This work was supported by the Office of Basic Energy Sciences, U.S. Department of Energy, under Grant No. DE-FG02-04-ER46108.

APPENDIX A: COMPUTING THE NUMBER VARIANCE VIA THE EPSTEIN ZETA FUNCTION FOR $d=12$, 16, and 24

Here, we summarize the steps in computing the asymptotic number-variance coefficient (34) for the lattices K_{12}, Λ_{16}, and Λ_{24}, which correspond to the densest lattice packings in dimensions 12, 16, and 24, respectively. Importantly, the sum in Eq. (34) converges slowly. We noted in Sec. III B that the dual of the lattice that minimizes the Epstein zeta function $Z_\Lambda(s)$ [defined by Eq. (35)] at $s=(d+1)/2$ among all lattices will minimize the asymptotic number-variance coefficient (34) among lattices. We will exploit number-theoretic representations of the Epstein zeta function that enable its efficient numerical evaluation and thus efficient computation of the asymptotic number-variance coefficient (34) using the aforementioned duality relation.

First, let us note that the Epstein zeta function $Z_\Lambda(s)$ (35) can be rewritten as follows:

$$Z_\Lambda(s) = \sum_{i=1} \frac{Z_i}{p_i^{2s}}, \tag{A1}$$

where Z_i is the coordination number at a radial distance p_i from some lattice point in the lattice Λ. (Note that the Epstein zeta function defined in this way applies to a general periodic point process provided that Z_i is interpreted in the generalized sense discussed in Sec. II.) The quantities Z_i and p_i for many well-known lattices in $\mathbb{R}^d$ can be obtained analytically using the *theta series* for a lattice Λ, which is defined by

$$\Theta_\Lambda(p) = 1 + \sum_{i=1}^{\infty} Z_i q^{p_i^2}, \tag{A2}$$

and is directly related to the quadratic form associated with the lattice [18]. This series expression can usually be generated from the simpler functions θ_2, θ_3, and θ_4, which are defined by [18]

$$\theta_2(q) = 2\sum_{m=0}^{+\infty} q^{(m+1/2)^2}, \tag{A3}$$

$$\theta_3(q) = 1 + 2\sum_{m=1}^{+\infty} q^{m^2}, \tag{A4}$$

$$\theta_4(q) = 1 + 2\sum_{m=1}^{+\infty} (-q)^{m^2}. \tag{A5}$$

Specifically, for the K_{12}, Λ_{16}, and Λ_{24} lattices, the associated theta series are given by [18]

$$\Theta_{K_{12}} = \phi_0(2q)^6 + 45\phi_0(2q)^2\phi_1(2q)^4 + 18\phi_1(2q)^6 = 1 + 756q^4 + 4032q^6 + 20\,412q^8 + \cdots, \tag{A6}$$

$$\Theta_{\Lambda_{16}} = \frac{1}{2}[\theta_2(2q)^{16} + \theta_3(2q)^{16} + \theta_4(2q)^{16} + 30\theta_2(2q)^8\theta_3(2q)^8] = 1 + 4320q^4 + 61\,440q^6 + \cdots, \tag{A7}$$

$$\Theta_{\Lambda_{24}} = \frac{1}{8}[\theta_2(q)^8 + \theta_3(q)^8 + \theta_4(q)^8]^3 - \frac{45}{16}[\theta_2(q)\theta_3(q)\theta_4(q)]^8 = 1 + 196\,560q^4 + 16\,773\,120q^6 + \cdots, \tag{A8}$$

where

$$\phi_0 = \theta_2(2q)\theta_2(6q) + \theta_3(2q)\theta_3(6q), \tag{A9}$$

$$\phi_1 = \theta_2(2q)\theta_3(6q) + \theta_3(2q)\theta_2(6q). \tag{A10}$$

Direct evaluation of Eq. (A1) has the same convergence problems as the direct evaluation of the asymptotic number-variance coefficient (34). However, we can exploit alternative number-theoretic representations of Eq. (A1) to facilitate its evaluation. In particular, there is an expression for the Epstein zeta function that can be derived using Poisson summation [19]:

$$F_\Lambda(s) = \pi^{-s}\Gamma(s)Z_\Lambda(s) = \frac{1}{s-\frac{d}{2}} - \frac{1}{s} + \sum_{\substack{\mathbf{p}\in\Lambda \\ \mathbf{p}\neq\mathbf{0}}} G(s,\pi|\mathbf{p}|^2) + \sum_{\substack{\mathbf{p}\in\Lambda^* \\ \mathbf{p}\neq\mathbf{0}}} G\left(\frac{d}{2}-s,\pi|\mathbf{p}|^2\right), \tag{A11}$$

where

$$G(s,x) = x^{-s}\Gamma(s,x), \tag{A12}$$

and $\Gamma(s,x)=\int_x^\infty e^{-t}t^{s-1}dt$ is the complementary incomplete gamma function. It is important to note that the volumes of the fundamental cells of the lattice and its dual associated with the first and second sums in Eq. (A11), respectively, are both taken to be unity here. Using the appropriate theta series given above for the lattices corresponding to the densest lattice packings for $d=12$, 16, and 24 and expression (A11) for $s=(d+1)/2$, one finds the corresponding Epstein zeta functions to be

$$Z_{K_{12}}(s = 13/2) = 12.527\ 470\ 092\ 112\ldots, \tag{A13}$$

$$Z_{\Lambda_{16}}(s = 17/2) = 2.606\ 378\ 060\ 701\ldots, \tag{A14}$$

$$Z_{\Lambda_{24}}(s = 25/2) = 0.026\ 464\ 258\ 871\ldots. \tag{A15}$$

Now since all of these lattices are self-dual (i.e., $K_{12}\equiv K_{12}^*$, $\Lambda_{16}\equiv\Lambda_{16}^*$, and $\Lambda_{24}\equiv\Lambda_{24}^*$), we can directly determine the corresponding asymptotic number-variance from (34) by replacing the sum therein with the appropriate evaluation of the Epstein zeta function specified by relations (A13)–(A15). The asymptotic number-variance values for $d=12$, 16, and 24 reported in Table II were obtained in this fashion.

APPENDIX B: INTERSECTION VOLUME OF THREE SPHERES IN THREE DIMENSIONS

For $d=3$, the intersection volume $v_3^{\rm int}(r,s,t;R)$ of three identical spheres of radius R whose centers are separated by the distances r, s, and t for $R>R_T$ is given by [62]

$$\begin{aligned} v_3^{\rm int}(r,s,t;R) = {} & \frac{Q}{6}rst + \frac{4}{3}\tan^{-1}\left(\frac{Qrst}{r^2+s^2+t^2-8R^2}\right) \\ & - r(R^2 - r^2/12)\tan^{-1}\left(\frac{2Qst}{-r^2+s^2+t^2}\right) \\ & - s(R^2 - s^2/12)\tan^{-1}\left(\frac{2Qrt}{r^2-s^2+t^2}\right) \\ & - t(R^2 - t^2/12)\tan^{-1}\left(\frac{2Qrs}{r^2+s^2-t^2}\right), \end{aligned} \tag{B1}$$

where $0\le\tan^{-1}x\le\pi$,

$$R_T = \frac{rst}{[(r+s+t)(-r+s+t)(r-s+t)(r+s-t)]^{1/2}} \tag{B2}$$

is the circumradius of the triangle with side length lengths r, s, and t and $Q=\sqrt{R^2-R_T^2}/R_T$.

[1] J. P. Hansen and I. R. McDonald, *Theory of Simple Liquids* (Academic Press, New York, 1986).
[2] S. Torquato, *Random Heterogeneous Materials: Microstructure and Macroscopic Properties* (Springer-Verlag, New York, 2002).
[3] F. H. Stillinger, H. Sakai, and S. Torquato, J. Chem. Phys. **117**, 288 (2002).
[4] D. Ruelle, *Statistical Mechanics: Rigorous Results* (World Scientific, Riveredge, NJ, 1999).
[5] S. Torquato and F. H. Stillinger, Phys. Rev. Lett. **100**, 020602 (2008).
[6] P. M. Chaikin and T. C. Lubensky, *Principles of Condensed Matter Physics* (Cambridge University Press, New York, 1995).
[7] A. Lang, C. N. Likos, M. Watzlawek, and H. Lowën, J. Phys.: Condens. Matter **12**, 5087 (2000).
[8] F. H. Stillinger, J. Chem. Phys. **115**, 5208 (2001).
[9] B. M. Mladek, D. Gottwald, G. Kahl, M. Neumann, and C. N. Likos, Phys. Rev. Lett. **96**, 045701 (2006).
[10] H. Cohn and A. Kumar, J. Am. Math. Soc. **20**, 99 (2007).
[11] S. Gravel and V. Elser, Phys. Rev. E **78**, 036706 (2008).
[12] M. A. Glaser, G. M. Grason, R. D. Kamien, A. A. Kosmrlj, C. D. Santangelo, and P. Ziherl, EPL **78**, 46004 (2007).
[13] O. U. Uche, F. H. Stillinger, and S. Torquato, Phys. Rev. E **70**, 046122 (2004).
[14] R. D. Batten, F. H. Stillinger, and S. Torquato, J. Appl. Phys. **104**, 033504 (2008).
[15] S. Torquato and F. H. Stillinger, Phys. Rev. E **73**, 031106 (2006).
[16] S. Torquato and F. H. Stillinger, Exp. Math. **15**, 307 (2006).
[17] A. Scardicchio, F. H. Stillinger, and S. Torquato, J. Math. Phys. **49**, 043301 (2008).
[18] J. H. Conway and N. J. A. Sloane, *Sphere Packings, Lattices and Groups* (Springer-Verlag, New York, 1998).
[19] P. Sarnak and A. Strömbergsson, Invent. Math. **165**, 115 (2006).
[20] H. Cohn and N. Elkies, Ann. Math. **157**, 689 (2003).
[21] T. C. Hales, Ann. Math. **162**, 1065 (2005).
[22] H. Cohn and A. Kumar, Ann. Math. **170**, 1003 (2009).
[23] S. Torquato and F. H. Stillinger, Phys. Rev. E **68**, 041113 (2003).
[24] The support of a function is the set of points where the function is not zero. A function has compact support if it is zero outside a compact set.
[25] D. Adickes *et al.*, IIE Trans. **34**, 823 (2002).
[26] R. Prix, Class. Quantum Grav. **24**, S481 (2007).
[27] L. Liberti, N. Maculan, and Y. Zhang, Optim. Lett. **3**, 109 (2009).
[28] R. Bose, *Information Theory, Coding and Cryptography* (McGraw Hill, New Delhi, 2002).
[29] Q. Du, V. Faber, and M. Gunzburger, SIAM Rev. **41**, 637 (1999).
[30] H. Reiss, H. L. Frisch, and J. L. Lebowitz, J. Chem. Phys. **31**, 369 (1959); this paper considered void nearest-neighbor functions for the special case of identical hard spheres in equilibrium Gibbs ensemble.
[31] S. Torquato, B. Lu, and J. Rubinstein, Phys. Rev. A **41**, 2059 (1990). This paper considered *two types* of nearest-neighbor functions void and particle quantities for a general "nonequilibrium" case of identical of spheres with arbitrary interac-

tions, e.g., spheres with variable interpenetrability that interact with repulsive and attractive forces.

[32] Mathematicians usually define a dual Bravais lattice to have a fundamental cell volume $v_{F^*}=1/v_F$ [i.e., without the factor of $(2\pi)^d$], in which case self-duality is defined with respect to unit density; see Ref. [18].

[33] A laminated lattice Λ_d in $\mathbb{R}^d$ is built up of layers of $(d-1)$-dimensional lattices in d-dimensional Euclidean space. Note that a general lattice has been denoted by Λ, which should not be confused with the specific laminated lattice Λ_d. This is the common notation for both objects, and therefore we adhere to this convention.

[34] S. Torquato and Y. Jiao, Nature (London) **460**, 876 (2009); Phys. Rev. E **80**, 041104 (2009). In these papers, the *asphericity* of a nonspherical solid body is defined to be ratio of the circumradius to the inradius of the circumsphere and insphere of the nonspherical particle, respectively, which provides a measure of the spherical asymmetry of a solid body. An asphericity equal to unity corresponds to a perfect sphere.

[35] C. A. Rogers, *Packing and Covering* (Cambridge University Press, Cambridge, England, 1964).

[36] C. E. Shannon, Bell Syst. Tech. J. **27**, 379 (1948).

[37] H. Minkowski, J. Reine Angew. Math. **129**, 220 (1905).

[38] S. Torquato, O. U. Uche, and F. H. Stillinger, Phys. Rev. E **74**, 061308 (2006).

[39] G. A. Kabatiansky and V. I. Levenshtein, Probl. Inf. Transm. **14**, 1 (1978).

[40] J. Beck, Acta Math. **159**, 1 (1987).

[41] C. E. Zachary and S. Torquato, J. Stat. Mech.: Theory Exp. (2009), P12015.

[42] R. A. Rankin, Proc. Glasg. Math. Assoc. **1**, 149 (1953).

[43] V. Ennola, Proc. Cambridge Philos. Soc. **60**, 855 (1964).

[44] P. Chiu, Proc. Am. Math. Soc. **125**, 723 (1997).

[45] A. Schürmann and F. Vallentin, Discrete Comput. Geom. **35**, 73 (2006).

[46] P. L. Zador, IEEE Trans. Inf. Theory **28**, 139 (1982).

[47] E. Agrell and T. Eriksson, IEEE Trans. Inf. Theory **44**, 1814 (1998).

[48] S. Torquato, Phys. Rev. Lett. **74**, 2156 (1995).

[49] S. Torquato, A. Scardicchio, and C. E. Zachary, J. Stat. Mech.: Theory Exp. (2008), P11019.

[50] For $d=1$, the condition on $H_V(0)$ in Eq. (55) should be replaced with $H_V(0)=2\rho$.

[51] S. Torquato, J. Stat. Phys. **45**, 843 (1986). The *canonical* n-point correlation function $H_n(\mathbf{x}^m;\mathbf{x}^{p-m};\mathbf{r}^q)$ is a *hybrid* probabilistic function in that it contains the character of a correlation function, probability function, and probability density function, depending on its arguments $(\mathbf{x}^m;\mathbf{x}^{p-m};\mathbf{r}^q)$ and the values of m, p, and q. From H_n, which has been explicitly represented as a series involving certain integrals over the n-particle correlation function g_n, one can derive any of the statistical descriptors that have arisen in the theory of random media and statistical mechanics as well as their generalizations. The reader is referred to Ref. [2] for a comprehensive discussion of H_n.

[52] There is an uncountably infinite number of periodic point configurations in $\mathbb{R}^d$ in which circumscribed overlapping spheres of radius $\mathcal{R}_c$ around each of the points just cover the space and render $E_V(\mathcal{R}_c)=0$ such that for $R>\mathcal{R}_c$. The point configuration that minimizes the support of $E_V(R)$, i.e., minimizes $\mathcal{R}_c$ (called $\mathcal{R}_c^{min}$) is the unique ground-state configuration or the optimal covering. Twice the covering radius $2\mathcal{R}_c$ for a particular point process determines the "effective range" of the interaction associated with $E_V(R)$; see the text for further explanation.

[53] B. Widom, J. Chem. Phys. **44**, 3888 (1966).

[54] A. Reńyi, Sel. Trans. Math. Stat. Prob. **4**, 203 (1963).

[55] J. Feder, J. Theor. Biol. **87**, 237 (1980).

[56] D. W. Cooper, Phys. Rev. A **38**, 522 (1988).

[57] Note that leading-order term in either Eq. (93) or Eq. (94) involving $1/2^d$ is a dominant dimensional contribution for RSA saturation densities in relatively low dimensions for good theoretical reasons [38]. The fact that this term does not appear in the upper bound (92) is another reason why it could only be realizable by RSA saturated packings in high dimensions. If true, then the $d\ln(d)$ and $d\ln[\ln(d)]$ terms in Eq. (92) are high-dimensional asymptotic corrections.

[58] Observe that the extrapolation of the conservative fit function (94) to $d=24$ gives a density that is about 3.7% larger than that predicted by Eq. (93). This percentage difference between the two fit functions decreases as d decreases to $d=7$.

[59] This includes the operational ground-based Laser Interferometer Gravitational-Wave Observatory and the space-based Laser Interferometer Space Antenna, which is expected to be operational in the next six years. See the link "Astro2010: The Astronomy and Astrophysics Decadal Survey."

[60] I. W. Harry, S. Fairhurst, and B. S. Sathyaprakash, Class. Quantum Grav. **25**, 184027 (2008).

[61] C. Messenger, R. Prix, and M. A. Papa, Phys. Rev. D **79**, 104017 (2009).

[62] M. J. D. Powell, Mol. Phys. **7**, 591 (1964).